AN INTEGRATED BEARING PROGNOSTICS METHOD FOR RE-MAINING USEFUL LIFE PREDICTION

TIANYI LIU

A THESIS

IN

THE CONCORDIA INSTITUTE

FOR

INFORMATION SYSTEM ENGINEERING

PRESENTED IN PARTIAL FULFILLMENT OF THE REQUIREMENTS

FOR THE DEGREE OF MASTER OF APPLIED SCIENCE (QUALITY SYSTEM ENGINEERING) AT CONCORDIA UNIVERSITY

MONTRÉAL, QUÉBEC, CANADA

May 2013

CONCORDIA UNIVERSITY

School of Graduate Studies

This is to certify that the thesis prepared

By: Tianyi Liu

Entitled: **An integrated bearing prognostics method for remaining useful life prediction**

and submitted in partial fulfillment of the requirements for the degree of

Master of Applied Science in Quality System Engineering

complies with the regulations of this University and meets the accepted standards with respect to originality and quality.

Signed by the final examining committee:

…Andrea Schiffauerova Dr. (Chair)

… ….WenFang Xie…… Dr. (External Examiner)

……..Chun Wang…… Dr. (Internal Examiner)

……Zhigang Tian…… Dr. (Supervisor)

Approved by _____

Chair of Department or Graduate Program Director

_____

Dean of Faculty

Date May 13, 2013

Abstract

An integrated bearing prognostics method for remaining useful life prediction

Nowadays, in order to improve the productivity and quality, more and more resources are invested in maintenance. In order to improve the reliability of an engineering system, accurate predictions of the remaining useful lifetime of the equipment and its key parts are required. Bearing plays an important role in the rotating machines. The purpose of using a bearing is to reduce rotational friction and support the load imposed on it in radial and axial directions.

The common types of bearing defects include damage in rolling elements, inner and outer races, etc. In this thesis, we focus on the spall propagation caused by rolling contact fatigue. The existing bearing prognosis methods are either model-based or data driven. In this thesis, we develop an integrated bearing prognostics method, which utilizes both physical models and condition monitoring data. In the physical model part, a Hertz contact model is used to analyze the stress developed from the contact point between two curved surfaces which are pressed together, the ball and the deep groove. Based on Paris' law, a damage propagation model is used to describe the spall propagation process. It is difficult to measure a defect size when the machines are running. Therefore, online data is obtained and processed to transform raw signals into useful information. In this thesis, the uncertainty factors are considered, including material uncertainty, model uncertainty and measurement error. A Bayesian method is used to update the distribution of this uncertainty factor by fusing the condition monitoring data, to achieve updated predictions of

remaining useful life.

Finally, two sets of data are used to verify and validate the proposed integrated bearing prognostics method. The first set of data includes a group of simulated bearing degradation histories. The second set of data were collected from lab experiments conducted using the Bearing Prognostics Simulator. These examples demonstrated the effectiveness of the proposed method.

The key contribution of this thesis is the development of an integrated bearing prognostics method, where the uncertain model parameters are updated using the collected condition monitoring data, while the existing bearing prognostics methods are either model-based or data driven. Both the development of the method and the experimental validation are significant contributions to the field of bearing prognostics.

Acknowledgements

First of all, I would like to acknowledge my supervisor Dr. Zhigang Tian successful completion of this thesis. His patience and encouragement will affect my whole life. I learned how to develop my knowledge and improve my research skills from him. He gives me the opportunity to work on real equipments during my research work. It is a valuable experience.

I also appreciate the help from all the Concordia Institute of Information System Engineering (CIISE) faculty, and people for their support. I would like to thank all the teachers who enrich my knowledge during my study period. I have gained a lot of knowledge and skills that will surely help me in my career.

Last but not the least; I want to thank my family for always supporting me. Without their emotional support, this hard work would not have been possible.

Table of Content

List of Figures

List of Tables

Acronyms

CBM	Condition Based Maintenance
R&D	Research and Development
RMS	Root Mean Square
ANN	Artificial Neural Network
RCF	Rolling Contact Fatigue
RUL	Remaining Useful Life
SIF	Stress Intensity Factor
STD	Standard Deviation
CF	Crest Factor
CM	Condition Monitoring
RPM	Revolutions Per Minute

Chapter 1

Introduction

In order to improve the reliability and reduce the operation cost, condition based maintenance (CBM) is widely used by modern manufacturers. As an important part of CBM and prognostics and health management, prognostics provide different approaches to predict the remaining useful life of the equipments or the parts.

Bearing plays an important role in the rotary machines to reduce rotational friction and to support the load imposed on it in radial and axial directions. In this thesis, we will try to establish an integrated method, which combines physical model and condition monitoring data, to predict the remaining useful life of bearings in a specific system.

1.1 Background

Nowadays, in order to improve productivity and quality, more and more money is spent on maintenance. Reliable production environment and accurate maintenance plan ensure high reliability and better quality. Manufacturers always make investment in R&D projects to develop new methods to achieve these goals. Normally, in a real production environment, no matter how high-quality the equipments and the related parts are, they will wear down over time. Therefore, in order to improve the reliability of the entire system, accurate predictions of the remaining useful lifetime of equipments and key parts are re-

quired.

Different production systems are running under different conditions. And even when they are operating under the same conditions, their lifespan most likely differ. Therefore, for a specific object such as bearing, the prediction of the remaining useful lifetime is difficult to make solely based on the historical data. Thus, a more accurate approach should be developed for these situations to improve the reliability level and reduce cost.

1.2 Condition based maintenance

Condition based maintenance is a maintenance strategy to optimize maintenance action based on condition monitoring data. As a type of preventive maintenance, the main purpose of CBM is to ensure production without unnecessary downtime.CBM is consisted of two areas, diagnostics and prognostics. Diagnostic is for fault detection. A good diagnostic method can detect the fault timely and accurately, and then maintenance can be implemented effectively. Prognostics is the prediction of the remaining useful life of equipments. CBM provides an optimal decision for maintenance action by using the condition monitoring data.

1.3 Research Motivations & Contributions

Reducing costs is always one of the main concerns of companies today. Every breakdown or replacement makes repair cost and unit cost go higher. More frequent routine mainte-

nance and replacement would certainly improve the reliability. But at the same time, it means more downtime and higher maintenance cost. The biggest challenge for making an optimal maintenance plan is to predict the remaining useful life of objects accurately.

The existing bearing prognosis methods are either model-based or data driven. However, both of them have many limitations. For physics model methods, in order to make the results accurately, we need to consider many parameters. On the other hand, data driven method need a huge historical data base to derive the prediction. These data need to be collected from a number of real experiments. It always takes time and does not take into consideration of the uncertainties.

In this thesis, an integrated method which utilizes both physical models and condition monitoring data will be proposed for bearing remaining useful life prediction under a certain condition. In the physical model part, a Hertz contact model is used to analyze the stress developed from the contact point between two curved surfaces which are pressed together, the ball and the deep groove. Based on Paris' law, a damage propagation model is used to describe the spall propagation process. Compared to the common physical model methods; this approach needs limited parameters

In this thesis, the uncertainty factors are considered, including material uncertainty, model uncertainty and measurement error. A Bayesian method is used to update the distribution of this uncertainty factor by fusing the condition monitoring data, to achieve refined predictions of remaining useful life. Finally, two sets of data are used to verify and validate the proposed integrated bearing prognostics method.

The key contribution of this thesis is the development of an integrated bearing prognostics method, where the uncertain model parameters are updated using the collected condition monitoring data, while the existing bearing prognostics methods are either model-based or data driven. Both the development of the method and the experimental validation are significant contributions to the field of bearing prognostics.

1.4 Thesis Organization

The other chapters of the thesis are organized as below:

In chapter 2, a literature review is given on the related methods of bearing diagnostics and prognostics.

In chapter 3, we introduce our integrated prognostics methods and related techniques, such as Hertz contact stress theory, Monte Carlo simulation, Bayesian theorem, and so on.

In chapter 4, we discussed how to use the proposed method. We use this integrated prognostics method with simulation degradation data to predict the remaining useful life of a bearing under a specific condition.

In chapter 5, two groups of experiments are carried out on a bearing prognostics simulator. The first experiment shows the existence of the uncertainties. The second experiment is used to validate the integrated method with real data.

In chapter 6, we draw conclusions from our research and discuss our future work.

Chapter 2

Literature Review

Bearings, a fundamental mechanical part, are widely used in modern industries. Application of rolling element bearings is to reduce rotational friction and support the load imposed on it in radial and axial directions. As we know, bearing plays an important role in a mechanical system, and even a small defect of the bearing can lead to a serious consequence. Thus, bearing failure is one of the foremost causes of breakdown in rotating machinery. In order to avoid the downtime and accidents, companies spend a lot on maintenance of bearings. It is necessary to predict its health condition accurately, to decrease the cost and increase the reliability of the whole system.

The common types of defect of bearing are pitting, surface damage, and rolling contact fatigue and so on. In this thesis, we will focus on the spall propagation caused by rolling contact fatigue (RCF).

This literature review is based on the previous research work on diagnosis and prognosis of rolling element bearing.

2.1 Bearing Diagnostics

Despite of the fact that bearings are not very expensive in a machinery system, their failure can cause disastrous consequences. Therefore, rolling bearing diagnostics has been studied by many researchers. With the increase in demand for higher reliability of real production systems, accurate fault detection is required. All the faults need to be detected

before they occur without interrupting the whole production process.

The main objectives of bearing diagnostics are to detect and identify the different types of faults or defects during operation. On the other hand, diagnostics can provide the data for prognostics.

For bearing diagnostics, the common methods are time domain and frequency domain analysis of signals. The main signals, such as vibration signals and acoustic emission signals are collected by specific sensors. In data processing step, we transfer the raw signal into some statistical features like root-mean-square (RMS), peak value, kurtosis value, and crest factor value and so on. Dyer and Stewart (1978) used a statistical parameter, Kurtosis value, to describe and analyze bearing condition signals. It is a fourth order deviation from mean. Price et al. (2001) analyzed the faults of bearings by combining acoustic emission signals and vibration data. Khemili and Chouchane (2005) proposed a method to clean noisy signal by filters. Choudhary and Tandon (1997) developed a model to find the relationship between the vibration frequencies and amplitude for rolling bearings.

The surface damage defect of bearing is normally caused by improper installation, misalignment of races or inadequate lubrication. Corrosion always occurs when water exists between bearing elements and leads to pitting on the surface of the bearing. These kinds of defect can be avoided by good operation method. A main failure of rolling bearings is spall propagation on the ball surface or race surface caused by contact fatigue (the spall is always initiated by a fatigue crack below the contact surface). Rosado et al. (2009) Nagaraj et al. (2009) Nelson et al. (2009) investigated the rolling contact fatigue initiation and

spall propagation characteristics of three different bearings. They showed the whole process of spall propagation by experiment. In fact, the experimental fatigue lives far exceed the calculated L_{10} life for bearings. In this thesis, we will focus on the spall propagation process.

2.2 Methods for predicting remaining useful life (RUL)

The estimations of traditional approach are based on event data. People estimate reliability and remaining useful life by analyzing the distribution of the event data such as replacement data and failure time historical data. The models such as Weibull distribution, Poisson distribution, Exponential distribution and Normal distribution have been used to analyze system reliability, especially Weibull distribution. Their common point is using historical time to failure data to estimate the reliability or mean-time-to-failure. Using this estimation, the manufacturers or engineers can make reasonable maintenance plan.

2.3 Prognostic approaches

The main models of prognostic are physics-based models and data driven models.

2.3.1 Physics-based models

Physics-based model uses mathematical models to describe the physical process of failure, such as defect growth and spall propagation. The most important theory of crack analysis is on Paris' formula, Li et al. (1999, 2000) developed a model to describe the relation between the crack growth rate and the defect area size, and used it on bearing prognostics. Kotzalas and Harris (2006) described the crack progress by their progression model. Based on the above methods, Kacprzynski et al. (2004) proposed a prognostic

method in terms of material factors and data fusion algorithms. The uncertainty in factors such as load and material properties limits the reliability of prognostics systems. The limitation of these models is that material constants are always determined empirically.

Li et al. (2005) used an embedded model, gear dynamic model (finite element model) to predict the RUL. The advantages of this model is that finite element analysis (FEA) enables stress calculation based on gear geometry, speed, load, material properties and so on. But this method takes time and needs expensive software to analyze the vibration data and calculate the stress value, and the results relies on the accuracy of the defect size.

Orsagh et al. (2004) provided a "comprehensive prognostics approach" for gas turbine engine bearings. This fatigue spall initiation and progression model can calculate the time to spall initiation and the time to failure under a defined condition. In order to obtain an ideal result, various physics parameters of this model should be determined accurately by numerical experiments.

Qiu et al. (2002) developed method for bearing lifetime prognostics based on damage mechanics. He considered the rolling bearing systems as a single-degree-of-freedom vibratory system. In the stiffness-based damage rule model, the natural failure frequency and the acceleration amplitude were related to the running time and failure time. In this model, the least-square scheme is similar to single-step adaptation in time series prediction. As Orsagh's models, various material constants need to be determined empirically.

Oppenheimer and Loparo (2002) proposed a Forman law crack growth model. It showed the relation between CM data and crack growth, and then predicted the useful life of

cracked rotor shafts. As the basic assumption is simplified, the usefulness of this model is limited. Table.1 summarizes the merits and limitation of Physics-based prognostics models.

Table 1 Physics-based models

Physics- based prognostics models		
Models	Merit	Limitation
Paris' law crack growth modeling	Model parameters can be changed in condition based on the least-square scheme.	a. Defect size is assumed to be linearly correlated to vibration RMS level. b. Empirical material constants.
Paris' law crack growth modeling with FEA	Stress can be calculated more accurately.(based on defect size, load, geometry and rotation speed)	a. Accurate crack size estimations are required. b. computationally expensive
Fatigue spall initiation and progression model	a. Calculates the time from spall initiation to failure. b. Cumulative damage can be estimated based on test condition	a. All the physics parameters should be determined by experiment as accurate as possible. b. Expensive measurement equipments
Damage rule model based on damage mechanics	Relates failure frequency and acceleration amplitude and running and failure time	Various material constants need to be determined accurately
Forman law crack growth modeling	Relates condition monitoring data and crack growth	More model parameters need to be determined for complex condition

Compare to the other methods, physics-based models have high performance with low cost. They also require less data than data-driven models.

2.3.2 Data driven models

Date driven models are built based on the historical data. They produce the prediction and

estimation based on CM data directly instead of building comprehensive physics-based model. The biggest advantage of data-driven methods is simple to calculate.

The common data driven methods are artificial neural network (ANN), hidden Markov method, auto-regression model, fuzzy logic and so on. ANN is widely used in data driven prognostic for rotary machines. For bearing systems, researchers always collect vibration or acoustic data by sensors for further research work. And then, all the data will be used to train the neural network to predict the results (failure time).

The simplest ANN-based prognostics approach is time series model. These models have the same points:

- Assume that failure occurs once the condition index exceeds the threshold;
- Assume that condition indices represent the actual asset health;
- Provide non-linear projection;
- Can estimate future time step.

Tian and Zuo(2009) proposed an extended recurrent neural network for health prediction of gearbox. Wang et al. (2001) developed a recurrent wavelet neural network to predict bearing crack propagation. Wang et al. (2004) developed a neuro-fuzzy network to predict spur gear condition. Tian et al. (2010) used ANN to predict the remaining useful life based on suspension histories and failure histories. They determined the optimal life prediction for each history data in order to minimize the validation mean square error.

Gebraeel et al. (2004) developed an exponential model to investigate the fatigue process of bearings in order to estimate the variation in bearings' life. They assumed that all bear-

ings degraded follow an exponential pattern. They analyzed single bearing and group of bearings networks with two models, trained one ANN for each historical dataset, and then predicted failure time based on the degradation signal data. These models estimate actual failure time instead of condition index at a future time period. Compared to the time series prediction, it has more accurate and realistic prediction by continuously engaging most recent condition data.

Jantunen (2004) developed a model for prognostic of rolling bearing failure. This model is based on regression analysis and fuzzy logic. It emphasizes the most recent condition data and fuzzy logic classifies the bearing health state based on historical data. It doesn't provide indication of time to failure or probability of failure. Zhang et al. (2007) proposed a model to estimate reliability based on condition data by using recursive Bayesian technique. This model estimates reliability using CM data of individual assets, rather than event data. The accurate results of this model rely on the correct determination of thresholds for various trending features. Zhang et al. (2005) developed a hidden Markov model. Their model can be trained to recognize different bearing fault types and states.

Data driven methods do not need to estimate the physics parameters. And also these methods are easy to handle and use without prior knowledge. However, because all the results are derived from the historical data, the inaccurate forecasts maybe produced in conditions of change. Therefore, most of these models assume that the monitoring system is stable. The estimation of future degradation on past degradation is generally required a large amount of data.

Table.2 summarizes the merits and limitation of data-driven models.

Table 2 Data-driven models

Data-driven models		
Models	Merit	Limitation
Time series prediction by ANNs	a. Easy to calculate b. Non-linear projection	a. shorten prediction horizon b. Failure occurs once the condition exceeds the presumed threshold.
Exponential model using ANN	a. Longer prediction horizon b. Estimates actual failure time	a. Assume all the bearing degradation follow an exponential pattern. b. Training one ANN for each dataset
Regression and fuzzy logic model	a. Emphasizes the recent condition information b. Fuzzy logic can classify conditions based on historical data.	Cannot predict time to failure or probability of failure
Recursive Bayesian	Estimate reliability by CM data of individual bearing	Requires an accurate determination of thresholds
Hidden Markov model	Recognize different bearing fault types by training	Prognosis relies on accurate threshold

2.3.3 Integrating reliability and CM data

While CM data are the main source of information for prediction of physics-based model, it always doesn't render reliability data. In order to obtain comprehensive and accurate prediction, several valuable models have considered integrating reliability data into prognostic. Goode et al. (2000) proposed a statistical approach to predict the remaining useful life of pumps. The “installation to potential failure” (IP) and the “potential failure to functional failure” (PF) intervals were represented using Weibull distribution. This method combines reliability and CM data to limit the factors affecting the time-to-failure predic-

tion. Then time to failure can be calculated in the PF interval taking into account vibration data.

Jardine et al. (1973, 1987, 1989, and 2006) applied the proportional hazards model (PHM) to estimate the reliability of bearing. They assumed that hazards changes proportionately with covariates. They also used Weibull distribution to model the baseline hazard function in PHM. EXAKT, a software which combining proportional hazards modes, transition probability and a cost model, was developed to calculate the optimal maintenance or replacement time intervals. Accurate transition probability calculation required a relatively large amount of CM historical data.

Sun et al. (2006) proposed a proportional covariates model (PCM) to estimate hazard functions of mechanical components even without historical failure data. They pointed out that the change in CM covariates is the reason of change in system hazard. Wang et al. (2002, 2005) developed conditional residual time distribution model and proportional residual model. These models only use the current asset condition information instead of the historical data to predict future asset health. All the tests were initially assumed to follow the Weibull delay time distribution model, as more CM data were obtained, the distribution was updated. This model requires the determination of a threshold level that indicates defect initiation. Satish and Sarma (2005) proposed a method which combines ANN and fuzzy logic to detect bearing condition. This method has the advantages of nonlinear mapping through ANN and condition classification through fuzzy logic. Wu et al. (2007) developed an integrated neural network which is based on decision support system to predict remaining useful life of bearings. Tian (2009) proposed a new ANN model to

make more accurate RUL prediction. This model takes the age and multiple condition monitoring parameters at discrete inspection points. In this model, both of current points and historical points are inputs and the life percentage is the output. He trained ANN with fitted measurement values (from failure history) and it provides more accurate prediction than Wu's model. Table.3 shows the merits and limitation of these models.

Table 3 Integrating reliability and CM data

Integrating reliability and CM data		
Approach	Merit	Limitation
IP and PF using Weibull distribution	Combines reliability and CM data to narrow down the distribution of time-to-failure	Requires an underlying distribution
Proportional hazards model	combines reliability and CM data to narrow down the distribution of time-to-failure	a. Accurate results depend on a large historical database b. PHM assumes the hazard changes proportionately with covariates (constant parameter)
Proportional covariates model	Do not require large historical failure data	Hazard changes proportionately with covariates by a fixed constant
Conditional residual time distribution model and proportional residual model	Takes all CM data into account	Hard to identify an accurate threshold that indicates the defect initiation
Intelligent estimator	a. Find out the relationship between the actual health and measurement data. b. Non-parametric	Requires large historical data for ANN training

2.4 Physics models

In this part, we will discuss the models which describe the spall propagation of ball bearing. RCF causes material to flake off from the contact surfaces of rolling elements and raceways. The positions of the spalls are located at a) Surface of the ball; b) Surface of the inner or outer raceways, as shown in Figure.1.

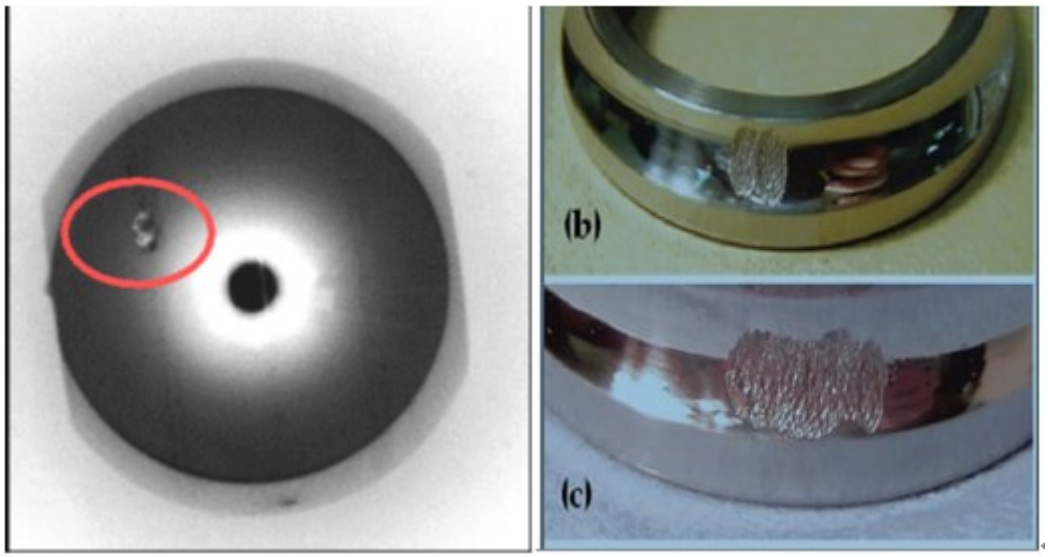

Figure 1 Spall

(a). *Spall on the ball* *(b),(c). Spall on inner surface (*Nagaraj et al. 2009*)*

As spall propagation grows in the bearing system and lead to failure, we need to define the spall propagation process, the relation between stress and defect. We also need to use related model to predict the remaining useful life of the bearing.

2.4.1 Kotzalas and Harris's model

While spall progression typically occurs more quickly than spall initiation, a study by Kotzalas and Harris showed that 3 to 20% of a particular bearings useful life remains after spall initiation. They analyzed two spall progression regions, stable and unstable spall

progression. Characteristics of stable spall progression are gradual spall growth and low broadband vibration amplitudes. The unstable spall progression has increasing broadband vibration amplitudes (Michael et al. 2008).

Kotzalas and Harris published an empirical method for estimation of friction within a failed ball–raceway contact. The results of their work indicated that the friction within a failed ball–raceway contact was not significantly larger than that of the unfailed contact for a significant period of time after initial spall.

The spall progression model by Harris (2001, 2006):

$$\frac{d_{Sp}}{d_N} = C(W_{sp})^m \tag{2.1}$$

$$w_{sp} = (\sigma_{max} + \tau_{avg})\sqrt{\pi S_p} \tag{2.2}$$

The model relates the spall progression rate (d_{sp}/d_N) to the spall similitude (Wsp) using two constants (C and m) as shown above. The spall similitude is defined in terms of the maximum stress (σ_{max}), average shearing stress (τ_{avg}), and the spall length (S_p).

In this model, two spall length measurements should be known (initial and final values). S_p is the spall size, N is the loading cycles. So d_{sp}/d_N shows the relationship between spall size (damage size) and time (N/rpm)

2.4.2 Damage Mechanics model

There are two key elements needed to model spall propagation: determination of dynamic loads and stresses occurring in the material as a rolling element passes over the spall, and

development of a method relating this local stress field to damage accrued in the material.

The stress field cannot be estimated by standard Hertzian contact methods since they assume ideal surface geometry, and the material missing from a spall creates a discontinuous contact area and significant impact forces. Numerical approaches are the only viable solution. A discrete damage mechanics model was developed by Marble et al. (2006).

The damage is the projected area of the defect (S_D) divided by the cross sectional area of the element (S). D is the damage size, a scalar value.

$$D = \frac{S_D}{S} \tag{2.3}$$

Defect reduces the effective area, thus increasing the effective stress.

$$\tilde{\sigma} = \frac{F}{S - S_D} = \frac{F}{S(1 - \frac{S_D}{S})} \tag{2.4}$$

Substituting D into the equation,

$$\tilde{\sigma} = \frac{F}{S(1-D)} = \frac{\sigma}{1-D} \tag{2.5}$$

D=0 means no damage; D=1 indicates a completely damage. In this equation, D is the percentage of the damage. We can assume value of D based on the damage level.

$$\frac{dD}{dN} = \frac{\sigma_E^2 C_{tr}}{2ES_E(1-D)^2}\varepsilon_E + \frac{\sigma_p^2 C_{tr}}{2ES_p(1-D)^2}\varepsilon_p \tag{2.6}$$

2.4.3 Model by Li

Li et al. (2000) published an empirical method for predicting spall progression rates for tapered roller bearings.

$$\frac{\mathrm{dD}}{\mathrm{dn}} = \mathrm{K}_1(\mathrm{D})^{\mathrm{K}_2} \tag{2.7}$$

K_1 and K_2 are empirical constants to be determined for all bearings and all operating conditions for which is used.

2.4.4 Model by Lundburg and Palmgren

Due to the stochastic nature of spall progression, the work of Lundburg and Palmgren (1947) was initially considered to model the spall progression phenomenon. Lundberg and Palmgren gave the probability of survival of an elemental volume $\mathrm{d_V}$ loaded by a nonchanging cyclic stress as

$$\frac{1}{\mathrm{S(n)}}\frac{\mathrm{dS(n)}}{\mathrm{dn}} = -\mathrm{g}[\Gamma(\mathrm{n})]\frac{\mathrm{d}\Gamma(\mathrm{n})}{\mathrm{dn}}\mathrm{dV} \tag{2.8}$$

It shows the relation between a beginning number of cycles $\mathrm{N_{start}}$ and an ending number of cycles $\mathrm{N_{end}}$ and using the Ioannides and Harris (1985) definition of the function G yields the following equation.

$$\ln\left(\frac{S(n_{start})}{S(n_{end})}\right) = A\left[\frac{T_{start}^{e} n_{start}^{e}}{z_{start}^{h}} - \frac{T_{end}^{c} n_{end}^{e}}{z_{end}^{h}}\right] dV \tag{2.9}$$

Spall progression isn't a continuous process. That is, when the spall progresses, the contact area and stress abruptly change, and then do not change until the next spall progression event. Because of this, the assumption that the stress criterion in the equation remains constant between spall progressions (T_{start}=T_{end}=T) was made.

$$n_{end} = \left\{ n_{start}^{e} + \frac{1}{A \int \ln\left(\frac{S(n_{end})\, T^{c}}{S(n_{start}) z^{h}}\right) dV} \right\} \text{^}(1/e) \tag{2.10}$$

$$S(n_{end}) = \exp\left\{ \ln\left(S(n_{end})\right) - \frac{AT^{c}}{z^{h}} (n_{end}^{e} - n_{start}^{e})\, dV \right\} \tag{2.11}$$

The equation above defines the number of cycles to cause a fatigue crack of critical size causing total failure within a given volume of material.

Chapter 3

The Integrated Prognostics Method

3.1 Framework of the integrated prognostics method

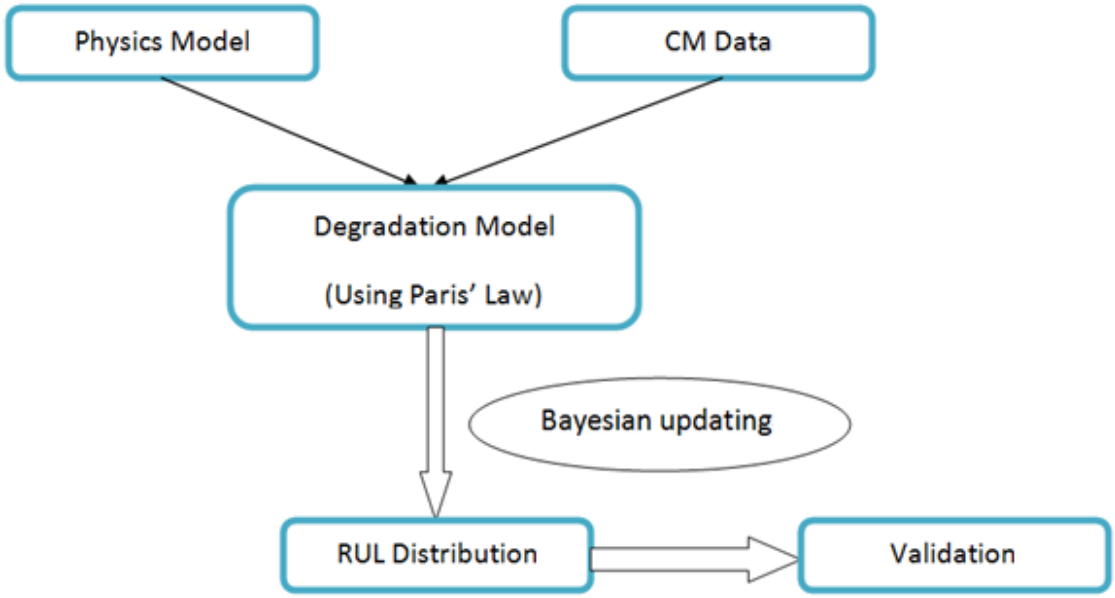

Figure 2 Main process of this integrated method

This framework, in Figure.2, shows the whole progress of this thesis. In the physics model part, we will determine all the parameters of the propagation model, including stress intensity factor (SIF), material parameter C and m. In the propagation model, the SIF is changed with the spall size overtime. We will use the formulas of the spall similitude to determine the values at different spall sizes. And then, SIF will be used in the degradation model which is based on Paris' Law. Then the failure time and the RUL distribution can be predicted considering the uncertainty of material parameter. On the other hand,

in the data-driven part, we will use a spall evaluation model to estimate the spall size by analyzing the condition monitoring data. The output of this model, the spall size, is seen as the real data. Then these real data can be used to update the distribution of the uncertainty (we will focus on material parameter m), and thus to get a more accurate prediction of RUL by keeping updating the parameters and condition estimation. The Bayesian updating method will be used for this purpose. Finally, we will validate the result by experiment.

3.2 Spall propagation model

Laboratory results indicate that fatigue defect growth is affected by a variety of factors such as stress states, temperature, operation error, measurement error, lubrication, and material parameters. The damage propagation models are used to describe the propagation progress. Most of the models are based on Paris' law, which consider the relationship between crack growth and stress. The following fatigue defect propagation model based on Paris' formula has been adopted for many years.

$$\frac{d_a}{d_N} = C_0(\Delta K)^n$$

Where a is the instantaneous defect size of a crack and N represents running cycles. C_0 and n are regarded as material-dependent constants, and are related to factors such as material properties. ΔK represents the range of stress intensity factor over one loading cycle. This model shows that crack growth rate per cycle is an exponential function of stress intensity factor range ΔK. In industry, the defect of a bearing is always represented by the spall size, rather than the length.

As we discussed above, once a spall initiates, it grows quickly with high vibration levels and high temperatures that finally lead bearing to failure. Because spall propagation occurs quickly and affects bearing useful life greatly, Kotzalas and Harris showed that bearing useful life had been shortened after spall initiation. In a stable environment, spall grows gradually with low vibration amplitudes. On the other hand, in unstable environment, the vibration amplitude increases.

Kotzalas and Harris developed a spall progression model, as Equation (2.1) and (2.2).

$$\frac{d_{Sp}}{d_N} = C(W_{sp})^m$$

$$w_{sp} = (\sigma_{max} + \tau_{avg})\sqrt{\pi S_p}$$

This model shows the relationship between

a). spall size (Sp) and loading cycle number (N);

b). the spall progression rate (d_{sp}/d_N) and the spall similitude (W_{sp}).

C and m are two material constants. The spall similitude, is defined by the maximum stress (σ_{max}), average shearing stress (τ_{avg}), and the spall length (Sp). They collected the data with a ball/v-ring test device. Only two spall lengths (initial and final value) were measured.

Although this model can describe the propagation progress, we always get the different failure times for different units (same type), even under the same condition. The uncer-

tainties such as human factors, operation factor and so on, which exist in these parameters are the main reasons. In this model, the parameters should have narrow distribution range when we take uncertainties into account. Once the distributions of the parameters are determined, we can predict the RUL more accurately. The condition monitoring data can be used to analyze the distributions of the parameters. In order to make it more accurate, Bayesian method will be used to update the distribution.

3.3 Determination of the model

In this thesis we will use this model to analyze the spall progression and then predict the RUL of the bearing. Firstly, we need to know all the values in the model such as maximum stress, average shearing stress based on our test condition. Then we will calculate the progression rate (d_{sp}/d_N). Finally, we will use integrated approach to predict the RUL.

Hertz contact stress theory is used to analyze the load capabilities and fatigue life in bearings. The contact stress is developed from the surface between two curved surfaces which pressed together. The area of contacts is divided into two types, point contacts (spheres) and line contact (cylinders). With load pressing, the whole environment constitutes the principal stresses of three dimensions. It causes the deformation (slightly) and development of a critical section below the surface of the bodies. Therefore, failure results in flaking or pitting on the surfaces of both bodies. Hertz contact stress theory gives the contact stress as a function. The curvature and modulus of elasticity of both bodies are important parameters.

In a ball bearing system, the type of contact is point contact. Consider two spheres held in contact by force F, their point of contact expands into a circular area of radius a, given

as.

$$a = \sqrt[3]{\frac{3F\left[\frac{1-v_1^2}{E_1}+\frac{1-v_2^2}{E_2}\right]}{4\left[\frac{1}{R_1}+\frac{1}{R_2}\right]}} \tag{3.1}$$

where E_1 and E_2 are the module elasticity for spheres 1 and 2. 'a' is the radius of the circular contact area. R_1 and R_2 are the radiuses of the two spheres. v_1 And v_2 are Poisson's ratios of the spheres. F is the force.

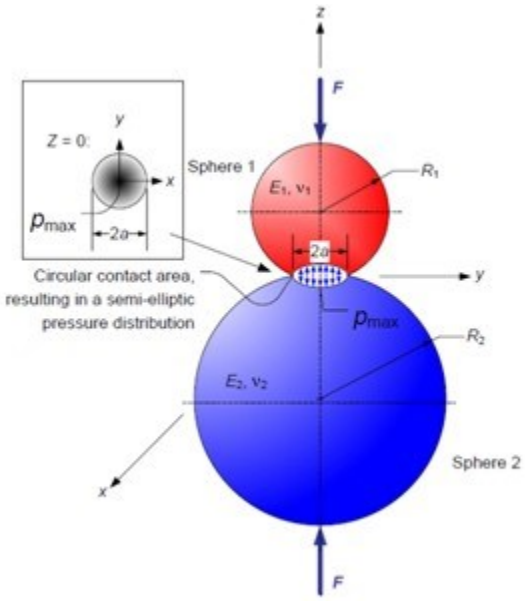

Figure 3 Spheres contact (Utah University)

This general expression for the contact radius can be applied to two additional common cases.

1. Sphere in contact with a flat plane ($d_2=\infty$);

2. Sphere in contact with an internal spherical surface or spherical groove (d_2=-d).

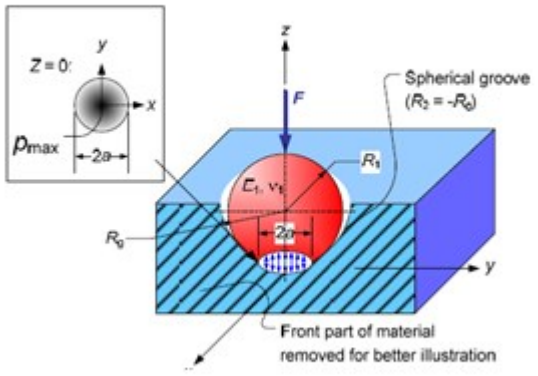

Figure 4 Deep groove contact (Utah University)

In Figure 3, 4, we can see that maximum contact pressure p_{max} occurs at the center point of the contact area is same as the two sphere cases.

$$P_{max} = \frac{3F}{2\pi a^2} \tag{3.2}$$

This is the maximum principal stress which is located at the center of the contact area. But material is compressed not only in the normal direction but in the lateral directions.The state of stress is computed based on the following mechanics.

1. Two planes of symmetry in loading and geometry dictates that $\sigma_x = \sigma_y$;

2. The dominant stress occurs on the axis of loading: $\sigma_{max} = \sigma_z$;

3. The principal stresses are $\sigma_1 = \sigma_2 = \sigma_x = \sigma_y$ and $\sigma_3 = \sigma_z$ given $\sigma_1, \sigma_2 >= \sigma_3$;

4. Compressive loading leads to σ_x, σ_y, and σ_z being compressive stresses.

$$\sigma_x = -p_{\max}\left[\left[1-\left|\zeta_a\right|\tan^{-1}\left(\frac{1}{\left|\zeta_a\right|}\right)\right](1+\nu)-\frac{1}{2\left(1+\zeta_a^2\right)}\right]$$
$$=\sigma_y=\sigma_1=\sigma_2 \tag{3.3}$$

$$\sigma_3 = \sigma_z = \frac{-p_{max}}{1+\zeta_a^2} \tag{3.4}$$

ζ_a=z/a is the non-dimensional depth below the surface (roller tilting angle). V is Poisson's ratio for the sphere examined (1 or 2).

$$|\tau_1| = |\tau_2| = \tau_{max} = \left|\frac{\sigma_1-\sigma_3}{2}\right| \qquad |\tau_3| = 0 \tag{3.5}$$

Many authorities theorize that the maximum shear stress is generated at ζ_a=0.48, meaning 0.48a below the sphere surface, and crack originates at the point of maximum shear, then progresses to the surface and make it pitting.

3.4 Uncertainty factor

Uncertainties always exist which are caused by human factor, operation, measurement and other unexpected errors. The accuracy of physics model is limited, because

- All models that describe the propagation progress only take the most important factors and parameters into account;
- The real process is more complicate than the assuming environment;
- In a machinery system, the uncertainty may be produced from the other related components.

All the uncertainties will affect the prediction of failure time and RUL directly or indi-

rectly. In order to reduce the effect of uncertainties and make the model more accurate, we need to consider the main uncertainties such as parameter uncertainty and model uncertainty. Firstly, we will take material uncertainty and model uncertainty into account, and then use Paris' law to predict the RUL. In the second step, update the prediction by adjusting the range of the value of uncertainty using Bayesian inference.

Material parameters C and m are important factors in this physics model. And the values of them are acquired by experiments with specific measurement equipment in controlled environment (for example, Kuna et al. (2005)). As we mentioned before, uncertainties of different factor have effect in the variations in the values of C and m. We assume that parameter C and m have normal distributions. In order to simplify the environment factor, this degradation model is based on simple Paris' law without considering other parameters.

An error term as model uncertainty, denoted by ε, is used to represent the difference between the real system mechanism and the result obtained by model. The modified model is written as.

$$\frac{dSp}{dN} = C(\Delta K)^m * \varepsilon \tag{3.6}$$

Measurement error τ is always produced in measurement process and estimation of spall size. The data of current spall size isn't measured and collected directly. We estimated it based on the sensor data using data processing, and thus the uncertainty is also associated with the estimation of the current spall size. So the real value a^{real} is assumed to follow normal distribution with mean (measured value) and standard deviation (τ).

$$a^{real} \sim N(a^{measure}, \tau^2)$$

3.5 RUL prediction

As mentioned above, the spall propagation is following the Paris' law. When the critical spall size a_c is reached, the bearing is broken. At a certain inspection point t, suppose that we know the mean of current spall size a_t with standard deviation, measurement error ε, we can obtain the predicted failure time distribution. We can modify Equation (3.6) as.

$$\frac{dN}{dSp} = \frac{1}{C(Wsp)^m * \varepsilon} \tag{3.7}$$

Wsp is the value of the stress intensity factor, obtained by Hertz contact theory.

Define the cycle number at the inspection point as N_i, then the total number of remaining useful cycles (can be converted to time) can be calculated by discretizing Paris' law.

$$\frac{N(i+1)-Ni}{a(i+1)-ai} = 1/\left[C(Wsp_i)^m * \varepsilon\right] \tag{3.8}$$

$$\overline{Wsp_i} = \frac{Wsp_i + Wsp_{i-1}}{2} \tag{3.9}$$

$$\frac{N(i+1)-Ni}{a(i+1)-ai} = 1/\left[C\left(\frac{Wsp(ai+1)+Wsp(ai)}{2}\right)^m * \varepsilon\right] \tag{3.10}$$

The sum of N_i, from the spall initiation to the critical spall size is reached, is the total remaining cycles, which can be converted as RUL. Due to fact that uncertainties exist in the whole process, we will use Monte-Carlo simulation to quantify these uncertainties in RUL prediction.

3.6 Monte Carlo simulation

Monte Carlo method is usually used in computer simulations of mathematical and physical systems. It is a computational algorithm to compute the values of parameters or probability by repeating random samples, especially when it is infeasible to compute an exact value with a deterministic algorithm. It is used to model phenomena with uncertainties in inputs. For example, it is difficult to compute the exact result of the spall propagation model even if we already knew the distribution of each parameter, such as C and m, because of the complexity of the calculation. Monte Carlo method can simulate the model and compute the predicted value. In order to increase the accuracy of the result, more simulation runs should be done.

Normally, we need to follow the procedures below:

- Develop a simple probability model or random model. This model should describe the real process.
- Based on the distributions of all the parameters, simulate the whole process by producing random parameters and repeating this procedure.
- Compute the random result
- Provide the probability distribution of the result. In this study, the result is RUL.

3.7 Prediction updating using Bayesian method

3.7.1 Bayes' theorem

Bayes' method shows the relationship between the probabilities of events A and B. For events A and B, the simple form is.

$$P(A|B)=\frac{P(B|A)P(A)}{P(B)} \tag{3.11}$$

P(A) and P(B) are the probabilities of A and B; $P(A|B)$ and $P(B|A)$ are the conditional probabilities of A given B and B given A. Bayes' theorem defines A and B as proposition and evidence respectively:

- P(A), the prior, is the initial degree of belief in A,
- $P(A|B)$, the posterior, is the degree of belief after B happen,
- P(B) is the normalized constant,
- $P(B|A)$ is the likelihood,

The prior is the probability of the event, represents what was estimated before obtaining the real data. The posterior is the conditional probability that is assigned after the relevant evidence is taken into account.

3.7.2 Bayes' Theorem for a given parameter 'θ'

When we have a prior belief that the probability distribution function is P (θ), and the observations data with the likelihood P (data | θ), then the posterior probability is defined as.

$$P(\theta|data) = P(data|\theta)\ P(\theta) / P(data) \tag{3.12}$$

In our study, the condition monitoring data contains specific information of the test bearing under the experiment conditions. The value of the spall size can be estimated at each time point. Thus, in order to get a more accurate result of RUL, we need to adjust and up-

date the parameters of the physical model.

For a large population of bearings, a widely distributed material parameter values exist. But for a specific bearing, the distribution of the parameter should be narrow. Thus, the new condition monitoring data provide a chance to reduce the uncertainty in these parameters.

We use Bayesian inference method to update the distributions of the material parameters. In order to simplify the situation, we only update parameter 'm'. The other material parameter 'C' is regarded as a constant.

The prior distribution of 'm' is $f_{prior}(m)$ and the likelihood to detect the real spall size is $l(a|m)$. Thus, the formula to calculate posterior distribution $f_{post}(m|a)$ is.

$$f_{post}(m|a) = \frac{l(a|m)f_{prior}(m)}{\int l(a|m)f_{prior}(m)dm} \tag{3.13}$$

For a fixed 'm', the likelihood to detect the real spall size at each inspection point is affected by two uncertainty factors, measurement error τ and model error ε. By discretizing Paris' law, the mean of the real spall size at the inspection point can be estimated by the previous spall size and stress intensity factor at the previous inspection point.

$$a_{j+1} = a[(i+1)\Delta N] = a(i\Delta N) + (\Delta N)C[Wsp(a(i\Delta N))]^m \varepsilon \quad i=j,j+1,\ldots. \tag{3.14}$$

We define ΔN as the increment of cycles. a_j is the estimated mean of spall size at inspection point j. It means we will inspect the spall size every ΔN cycles, which can be controlled by time. Then the new spall size should be.

$$a_{j+1}^{real} \sim N(a_{j+1}, \tau^2) \tag{3.15}$$

Based on central limit theory, the value of model error ε relies on its mean. Therefore, a_{j+1} is treated as a constant instead of a distribution due to model error. The PDF of the real spall size due to measurement error, is defined as g(a). The probability to get the real spall size of a_j is determined by $g(a_j)$.

3.7.3 Prior distribution of m

Different bearings may have different parameters 'm'. Based on this situation, m follows a statistical distribution, denoted by N_1. But for a specific bearing being monitored, the distribution of m should be very narrow or even close to a fixed value, denoted by N2. Because of the uncertainties, the value is difficult to determine accurately. So as mentioned before, we use condition monitoring data, which can reflect the property of the bearing, to update the distribution of m from a prior value then to get a posterior value.

To determine the prior for m, first, we need a set of degradation paths of different tested bearings from historical data, denoted by P, and each path corresponding to bearing i ϵ P. And then, in order to obtain the prior distribution of m, we will estimate the material parameter m for each bearing based on these historical data. For path i, we need to collect the spall size data at specific inspection point j, and denoted by a_j^{mea},j=1,…M. The second step, we generated a group of simulation data to describe the spall propagation process, denoted by $a^{app}(m)$, corresponding to parameter m using Equation (3.14), taking both model error and measurement error into account. We collected the spall size data from each bearing at the same inspection point $INSP_j$, j=1…M, and the simulated spall

size values are $a_j^{app}(m)$, j=1…M. Hence, at a specific inspection point, the difference between the actual value and the simulated value is, $e_j(m) = a_j^{mea}(m)-a_j^{app}(m)$. We can obtain the optimal material parameter value, denoted by m_{op}, by minimizing the difference between the two values, in the actual paths and simulated paths. We used the mean of least-square criteria to optimize it. And then, the optimal material parameter 'm' for path i, should satisfies.

$$\sum_{j=1}^{M}(e_j(m_{op}^i))^2 \leqslant \sum_{j=1}^{M}(e_j(m))^2 \tag{3.16}$$

Third, we fit the optimal material parameter values for all tested bearings by normal distribution. We can obtain the mean μ_{prior}^m and standard deviation σ_{prior}^m for the prior distribution of 'm'. Thus, the PDF of prior distribution of m becomes:

$$f_{prior}(m) \sim N(\mu_{prior}^m, {\sigma_{prior}^m}^2) \tag{3.17}$$

Last, after getting $f_{prior}(m)$, we can update the distribution of the material parameter m by Bayesian method when the condition monitoring data is collected.

Chapter 4

Numerical Examples

In this section, we use simulated degradation paths to illustrate the proposed integrated prognostic method. The related parameters of the bearing models are the same as those in the bearing prognostics simulator in our lab.

4.1 Conditions of the experiment

Normally, the historical bearing failure data was produced from a real industrial environment. However, it will be a time consuming process. In order to reduce the total duration, we need to accelerate the failure process. Two parameters are set as 1). Load in radial direction, 2500lbf; 2). High constant rotation speed, 2000 RPM. In these tests, the factors like load, rpm, and temperature etc, fixed from the beginning to the end.

With this test condition, which is higher than the normal operation condition, the spall will be initiated after only few hours. The spall is located at the surface of one ball. When the critical spall size is reached, the experiment is finished.

The parameters of the test bearings are given as follows:

a). Bearing: SKF 6205-2RSH Deep groove ball bearings (shown in Figure.5), single row, with solid oil, seal on both sides.

Figure 5 SKF 6205 Ball bearing

b). The detail information of specification is shown in Figure.6.

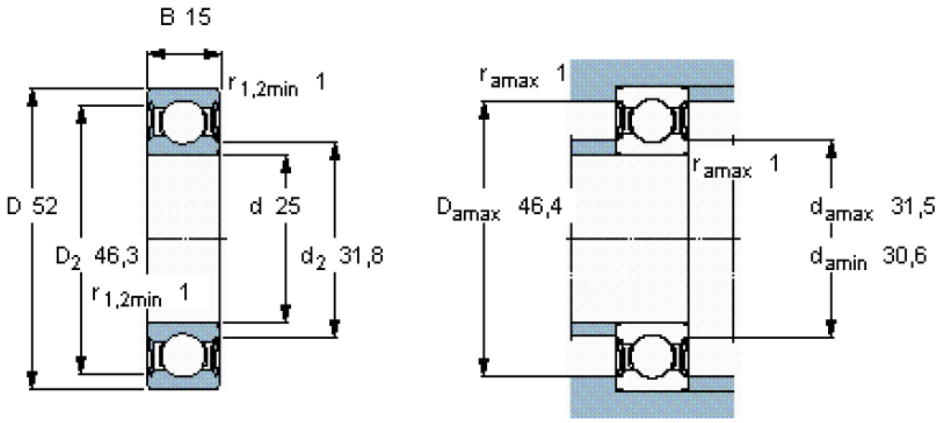

Outer ring O.D. D		Groove dia. max. D_3	
mm	in	mm	in
40	1.5748	38.10	1.500
47	1.8504	44.60	1.756
52	2.0472	49.73	1.958

Figure 6 Detail information of SKF 6205 (SKF Canada limited)

The radius of the balls is 3mm and that of the groove is 24.8mm, denoted by R_1 and R_2, respectively. Based on experimental observations, we suppose the critical spall size is around 15 mm^2 .

c). The parameters of the materials: Poisson's ratio is 0.3 (for steel); the elastic modulus is 300GPa.

Using Hertz contact theory; we calculate the related W_{sp} value. For simplicity, Poisson's ration of ball and groove v_1 and v_2 are taken as 0.3 in the following equations. The Equation (3.1) becomes

$$a = 0.88 * \left(\frac{F(E1+E2)R1R2}{E1E2(R1+R2)}\right)^{1/3} \tag{5.1}$$

We assume that the material of the ball and groove is the same, substituting R_2=-R_2. We obtain the following equations.

$$a = 0.88 * \left(\frac{2F*R1R2}{E(R2-R1)}\right)^{1/3} \tag{5.2}$$

$$P_{max}x = 0.623 * [FE^2(\frac{R2-R1}{2R1R2})^2]^{1/3} \tag{5.3}$$

From Equation (5.2) and (5.3), we obtained the values of a and P_{max}.

a=0.6223mm

P_{max}= 1.38GPa

From Equation (3.3) and (3.4), we obtain the values of σ_1,σ_2,σ_3, σ_x,σ_y and σ_z

$$\sigma_1=\sigma_2=\sigma_x=\sigma_y=-0.266\text{GPa}$$

$$\sigma_3=\sigma_z=-1.12\text{GPa}$$

From Equation (3.5),

$$\tau_1=\tau_2=0.427\text{GPa} \quad \tau_3=0$$

Figure.7 shows the relationship between W_{sp} and spall size.

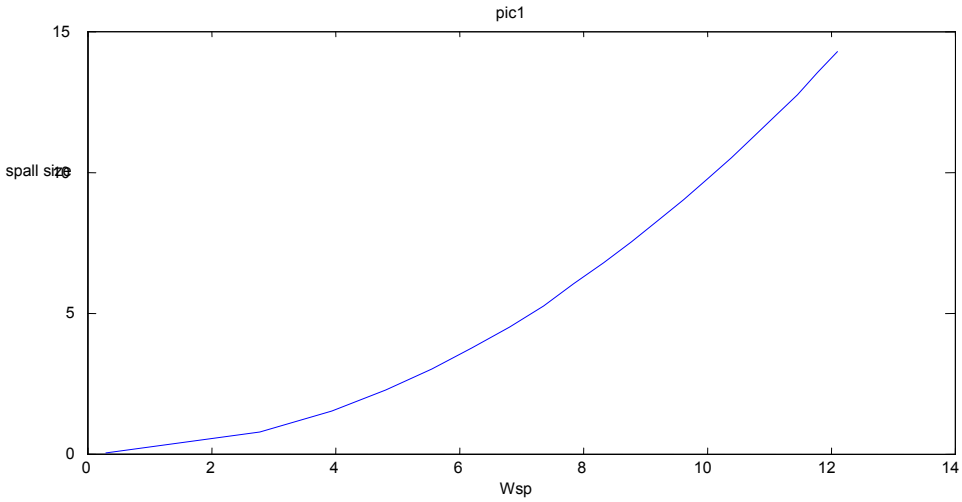

Figure 7 The values of W_{sp} at different spall size

Now we can use these values in the spall propagation model. For steel, we assume that the values of material parameters C and m are 0.95E-11 and 3, and the initial spall size is 0.01mm².

4.2 Example using simulated degradation path

In this example, we only update parameter m, and the other material parameter C is assumed to be a constant when generating these paths.

For each path i, the parameter m_i is defined as a random sample from the population distribution N_1 (3, 0.2), and the value is fixed until the bearing is broken. Model error ε follows normal distribution. At each inspection time, the value of spall size is generated by Equation (3.14) plus random deviation caused by measurement error τ. These paths are divided into two parts, training set and test set. The training set is used to define the prior distribution for m and the test set is used to validate the result and method.

In these degradation paths, the related values and distributions are shown in Table.4.

Table 4 Parameters of test

	Description	Value
C	Material parameter	9.50E-11
τ	Measurement error	0.2
m	Material parameter	N(3,0.2)
ϵ	Model error	N(3,0.3)

Base on Equation (3.14), we generate 10 degradation paths, shown in Figure.8, with spall size from initial size 0.01mm² to failure size 15mm².For each path i in training sets, the optimal value of m, m_i^{op}, i=1,2…7, satisfying the Equation (3.16) can be obtained by optimization. Through training, seven values of m were obtained. By fitting these values in normal distribution, we obtained the prior value of m.

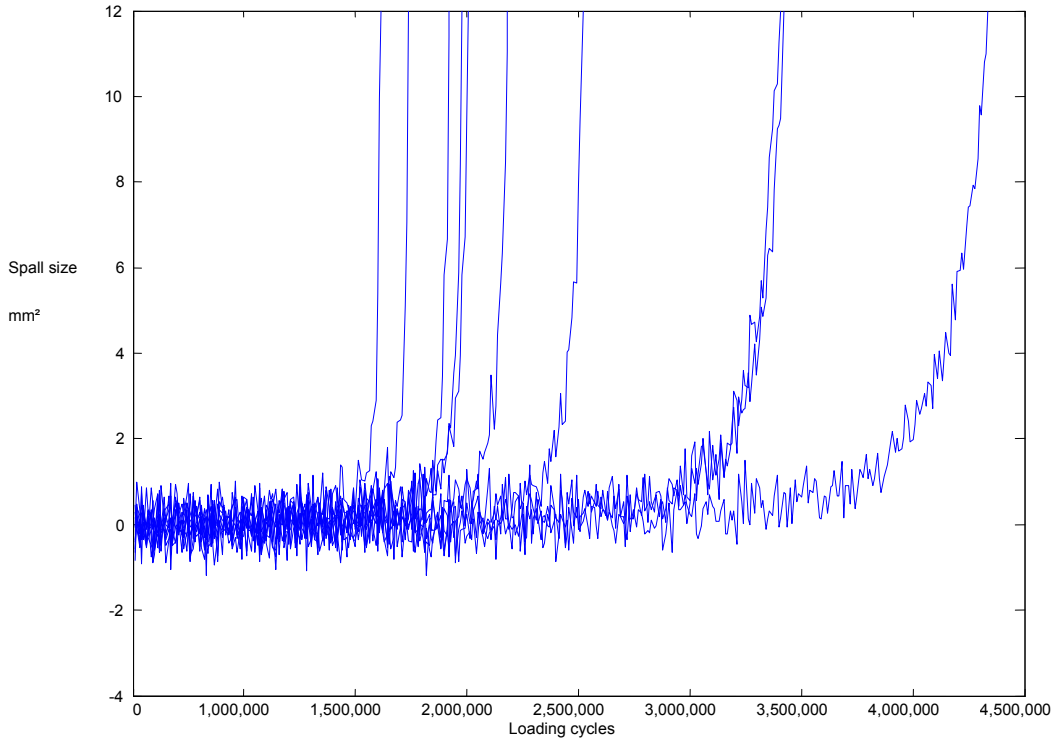

Figure 8 Ten degradation paths

Table 5 shows the values of m. The values on the left were used to generate the ten degradation paths. Seven trained values are generated to find out the prior distribution of m by fitting them in normal distribution.

$$f_{prior}(m) \sim N(3.0712, 0.1107^2)$$

Then we use 3 paths #8, #9, #10 to validate the integrated bearing prognostics method. At each inspection point for updating, the posterior distribution of m will become the prior distribution for the next interval.

Table 5 The real values and trained values of m

Path	Real value	Trained value	Trained err
1	3.00518	3.00508	0.04724
2	3.16193	3.1632	0.0766
3	2.91813	2.9405	0.09446
4	3.1816	3.18215	0.04385
5	3.09653	3.09607	0.04258
6	3.15289	3.1498	0.03971
7	3.20326	3.19487	0.05417
8	2.9381		
9	2.82609		
10	3.11276		

For path #8, the total number of loading cycles, that is, the failure time is 3.67e6 cycles. The real value of m is 2.938. The related values and updating process are shown in Table 6 and Figure.9.

Table 6 Related values of test #8

updating point	spall size	mean of m	std of m
0	0.01	3.0712	0.1107
6.00E+05	0.375	3.03	0.0497
1.20E+06	0.45	2.9074	0.0142
1.80E+06	0.363	2.8792	0.0102
2.40E+06	1.26	2.9308	0.089
3.00E+06	6	2.9364	0.003

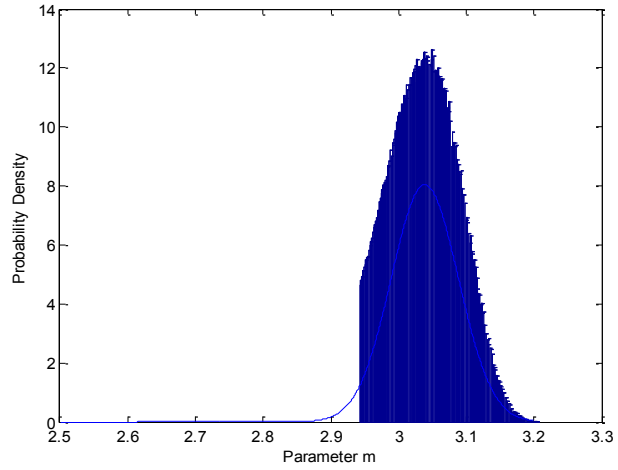

(a)

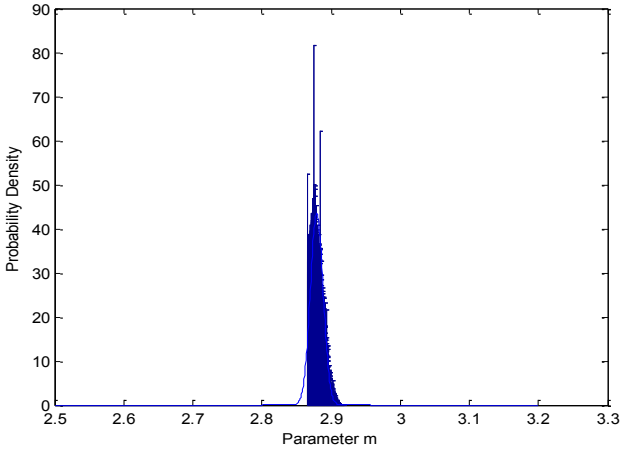

(b)

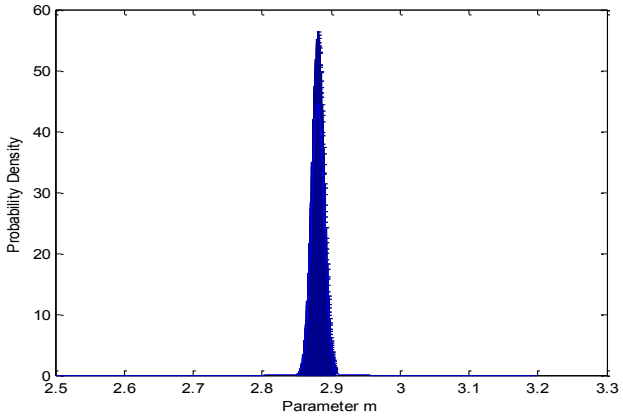

(c)

Figure 9 Updating process for test #8

(a) 1st update (b) 2nd update (c) 3rd update

For path #9 and #10, the total numbers of loading cycles are 4.4e6 and 1.95e6, respectively. The details and parameters of updating process are shown in Table.7.

Table 7 Related values of test #9

updating point	spall size	mean of m	std of m
0	0.01	3.0712	0.1107
3.00E+05	0.2505	3.24	0.0957
6.00E+05	0.2445	3.0697	0.0594
9.00E+05	0.312	3.0685	0.058
1.20E+06	0.3345	3.0458	0.0538
1.50E+06	0.4545	3.0349	0.0512
1.80E+06	0.5625	3.0175	0.0474
2.10E+06	0.684	2.9953	0.0421
2.40E+06	1.44	2.9014	0.0252
2.70E+06	1.6875	2.9249	0.0246
3.00E+06	2.694	2.8527	0.0017
3.30E+06	4.764	2.8499	0.0013

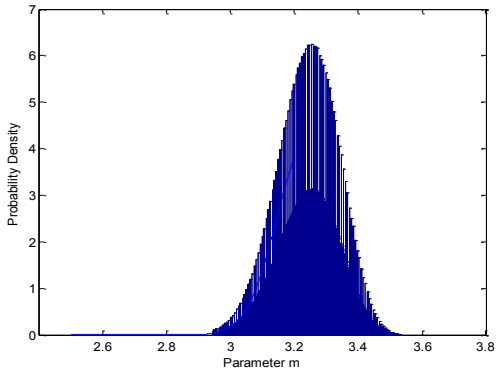

(a)

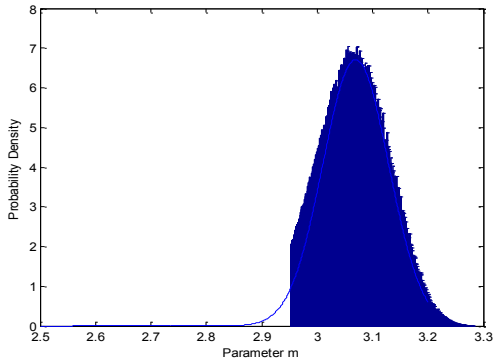

(b)

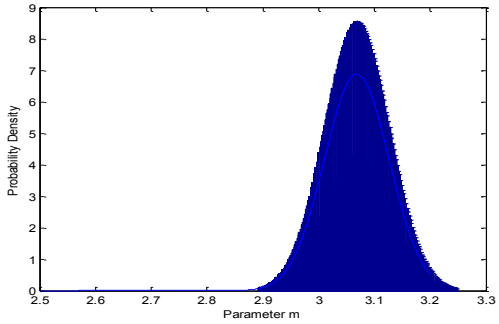

(c)

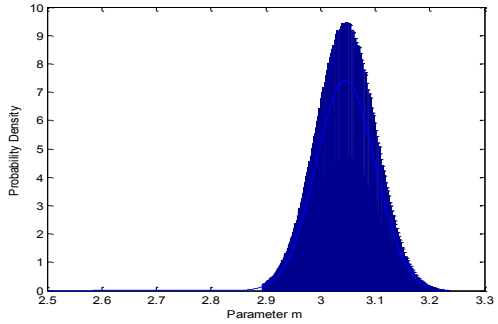

(d)

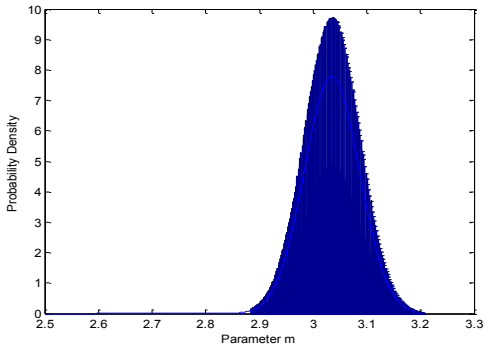

(e)

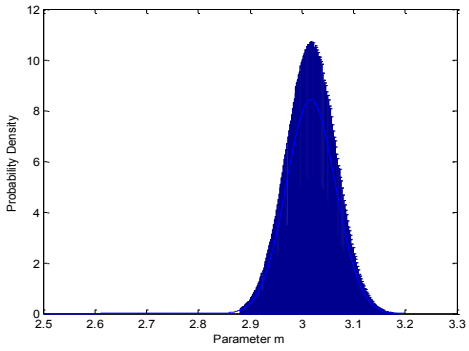

(f)

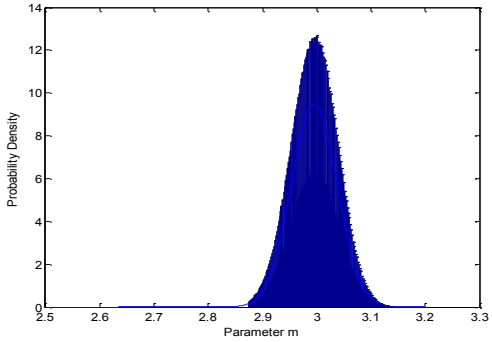

(g)

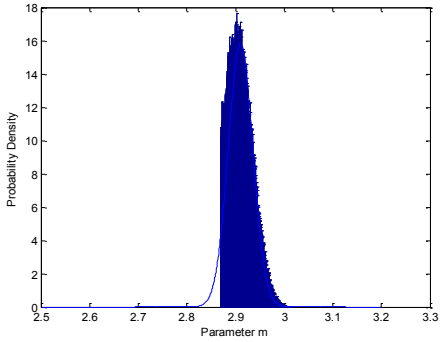

(h)

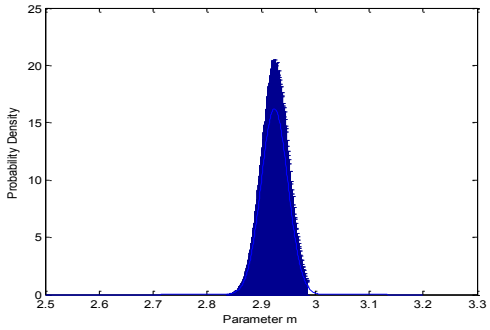

(i)

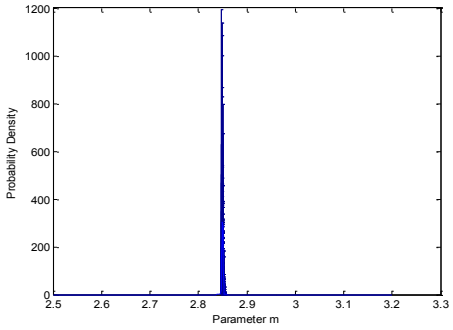

(j)

Figure 10 Updating process for test #9
(a) 1st update (b) 2nd update (c) 3rd update (d) 4th update (e) 6th update
(f) 7th update (g) 8th update (h) 9th update (i) 10th update (j) 11th update

We also shorten updating intervals in path #9 from 6e5 to 3e5. The corresponding results are shown in Figure.10. After updating 11 times, the accuracy is similar to path #8 (updated 5 times), shown in Figure.9. In path #10, we also use the same updating plan as path #9, updated every 3e5 cycles. The related values are shown in Table.8 and Figure.11.

Table 8 Related values of test #10

updating point	spall size	mean of m	std of m
3.00E+05	0.1685	3.0712	0.1107
6.00E+05	0.2090	3.0379	0.0980
9.00E+05	0.3867	3.0526	0.0981
1.20E+06	0.4855	2.9406	0.0726
1.50E+06	0.8513	2.9618	0.0733
1.80E+06	2.7860	3.1032	0.0076

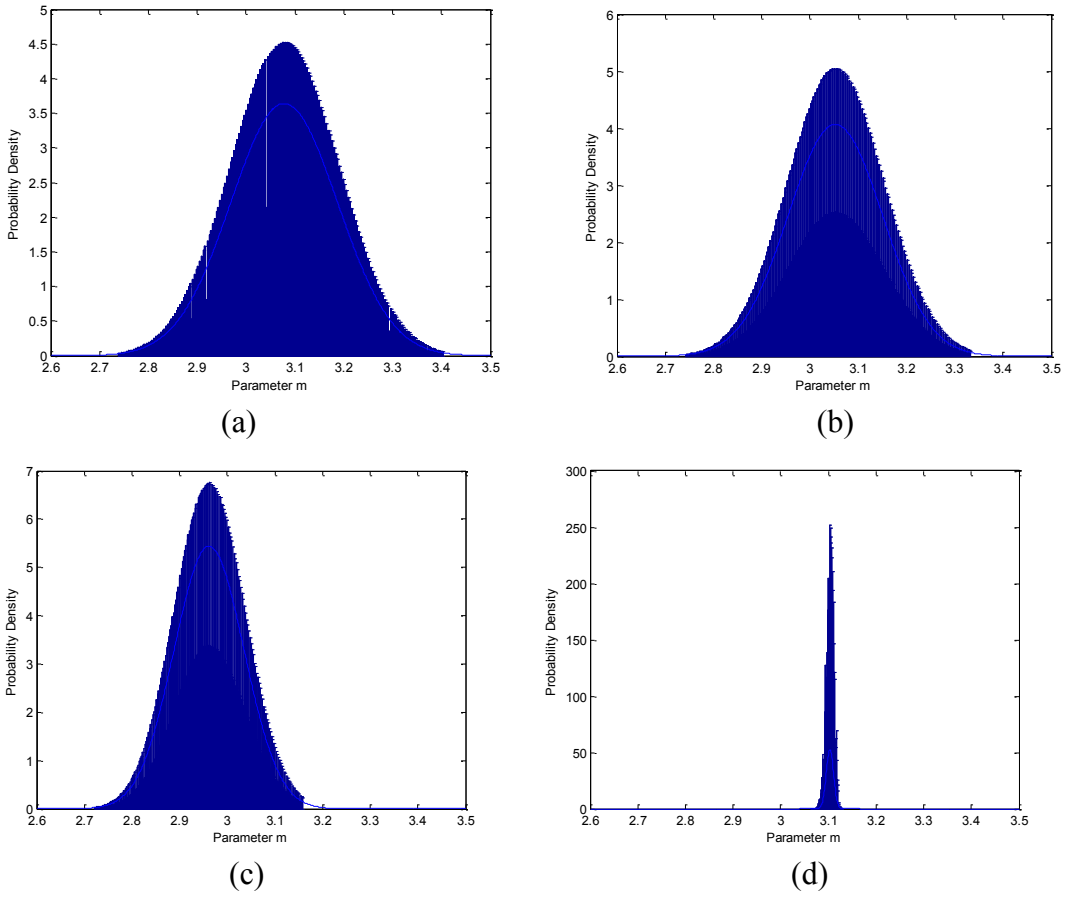

Figure 11 Updating process for test #10

(a) 1st update (b) 3rd update (c) 5th updates (d) 6th update

Table 6, 7 and 8 show us the updating process. It keeps updating the mean of m and reducing its standard deviation. As a result, the mean value of m, from its initial value

3.0712 approaches the real value, when the condition monitoring data at each updating point are used. From the figures, the distribution of m becomes narrower gradually. Moreover, the standard deviation of m is reduced after applying the updating approach. As the result of the exponential form of Paris' law, RUL is very sensitive to the value of m. Even with a small change in m, the result of RUL becomes very different.

The predictions of failure time for these paths, #8 #9 and #10, are shown in Table.9.

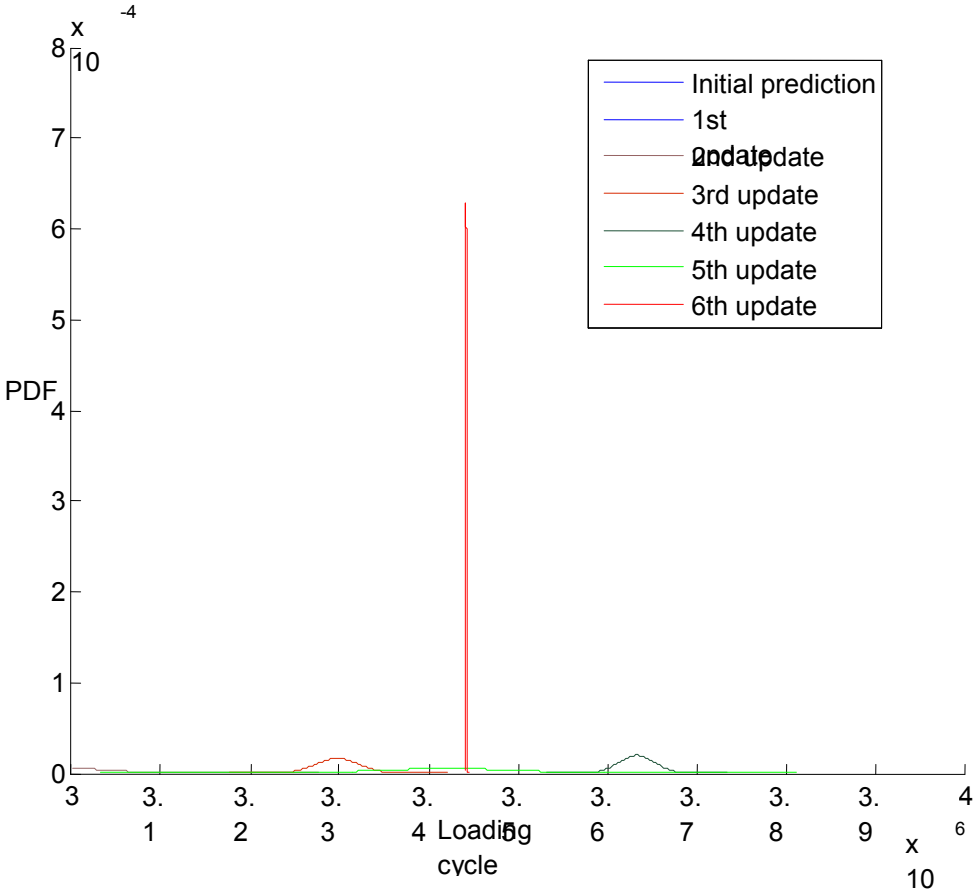

Figure 12 RUL prediction of test #8

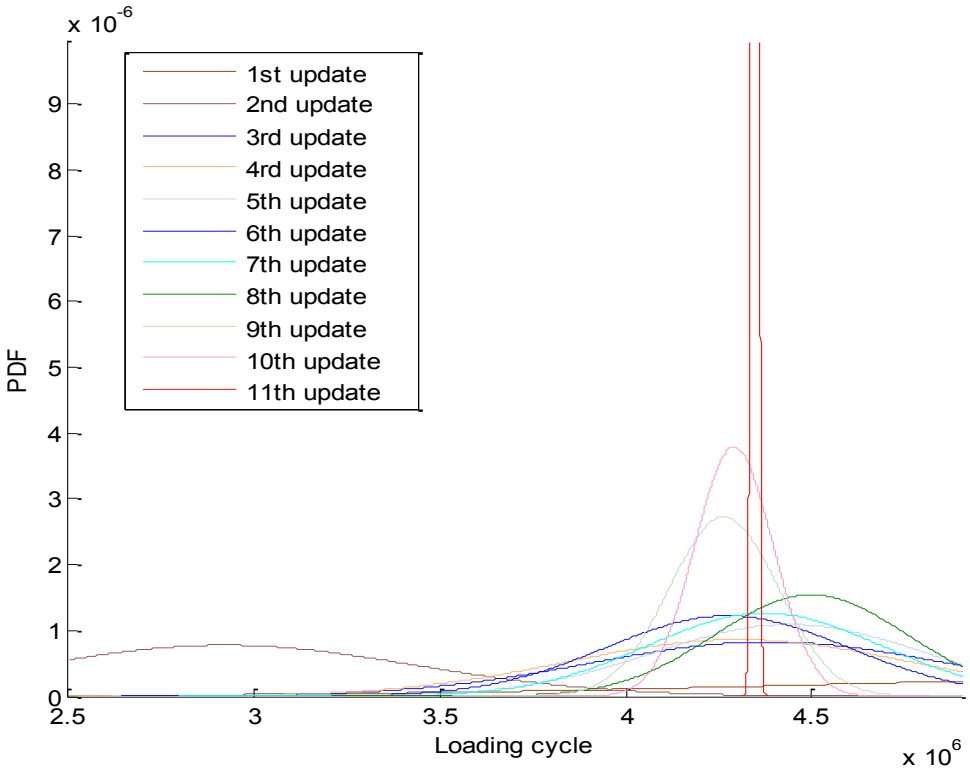

Figure 13 RUL prediction of test #9

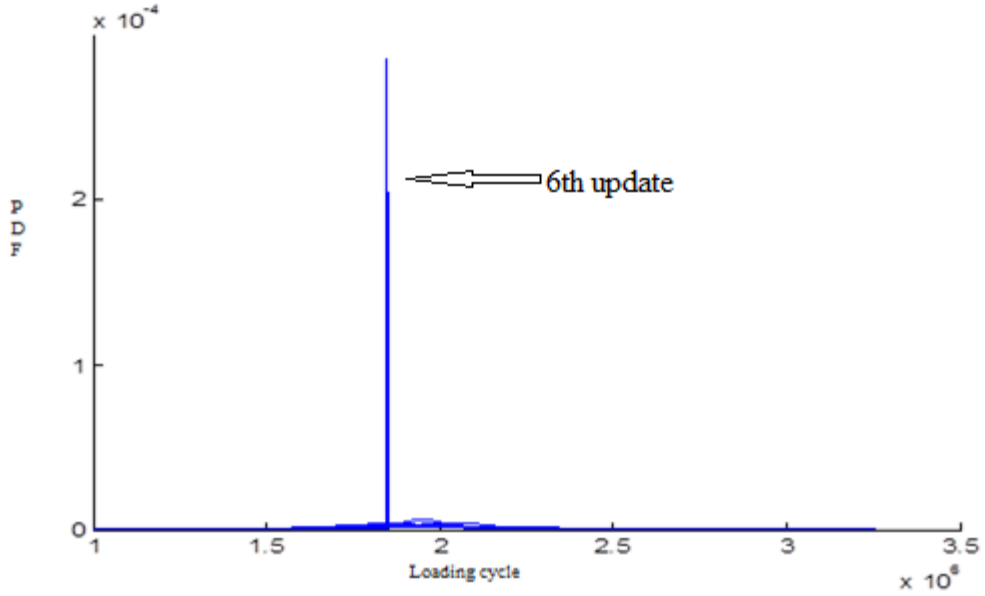

Figure 14 RUL prediction of test #10

Table 9 The real RUL and the predicted RUL

Path	Real RUL	prediction
8	3.67E+06	3.45E+06
9	4.40E+06	4.34E+06
10	1.95E+06	1.84E+06

From Figures. 12, 13 and 14, we can see that the prediction of failure time distribution becomes closer to the real failure time.

Comparing to the normal data-driven prognostics approaches, the significant advantage of this integrated method is that it predicts based on less historical data.

Chapter 5

Experimental Validation

In this chapter, we validate the proposed integrated bearing prognostics method by experiments. This chapter contains the description and detail information of the experiment, such as test plan, related equipments, test condition, software and the validation results. Two groups of experiments were carried out on a bearing prognostics simulator. Experiment 1 is used to show the existence of the uncertainties and collect historical data for experiment 2.

5.1 Bearing prognostics simulator

Figure 15 The bearing prognostics simulator

Bearing Prognostics Simulator (BPS), as shown in Figure.15, is used to perform bearing run-to-failures experiment. It is possible to accelerate the propagation process by applying high load. This test system can be driven in a constant rotational speed. This system provides an opportunity validate the prediction model of remaining useful life based on routine condition monitoring data.

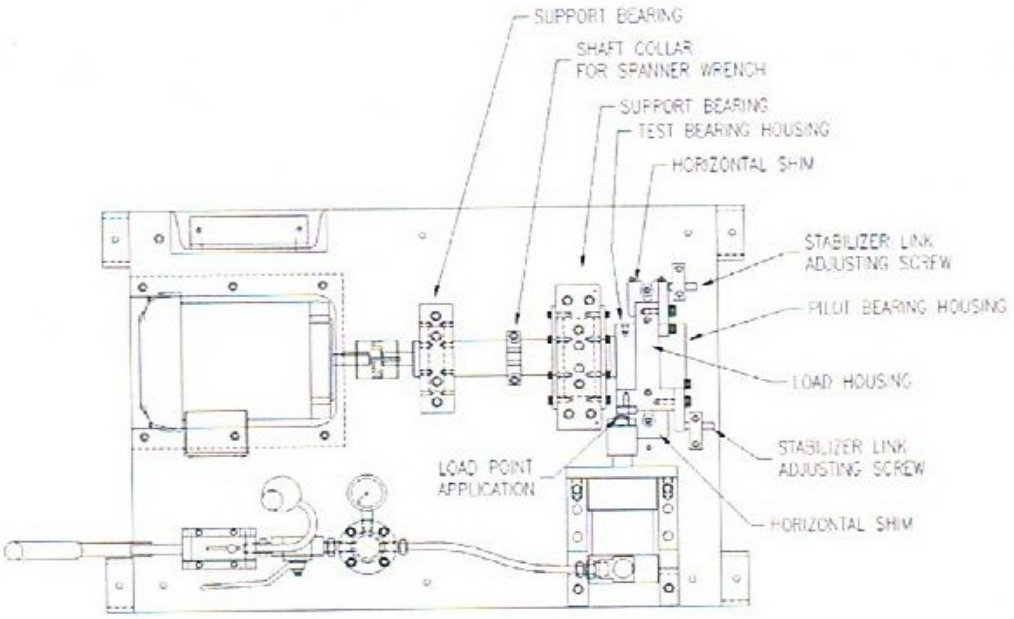

Figure 16 BPS overall schematic (Spectra Quest, Inc.)

5.2 Subsystems

As shown in Figure.16, the BPS system consists of four main subsystems:

- The motor and its controlling system
- The hydraulic loading system
- The bearing shaft rotating system
- The transducers and data acquisition system

The motor and controller are designed to control the rotation speed of the bearing shaft system. For our experimental plan, the BPS system runs at a constant rotation speed, 2000 rpm. The controller is shown in Figure.17.

Figure 17 Controller

The hydraulic load system, shown in Figure.18, generates 500 lbf per 100 psi. A radial load can be applied at the test bearing from a load point.

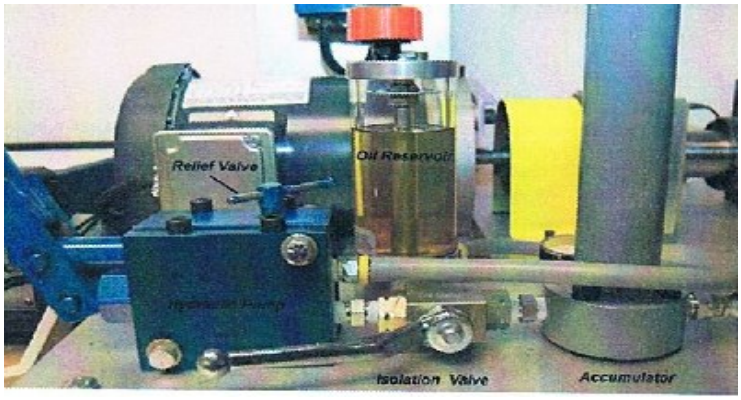

Figure 18 BPS hydraulic loading system

The test bearing is installed on the shaft and mounted in the housing. The outer race is stationary and fixed to the housing. The inner race is fixed to the shaft. Installation is shown in Figure 19.

(a)

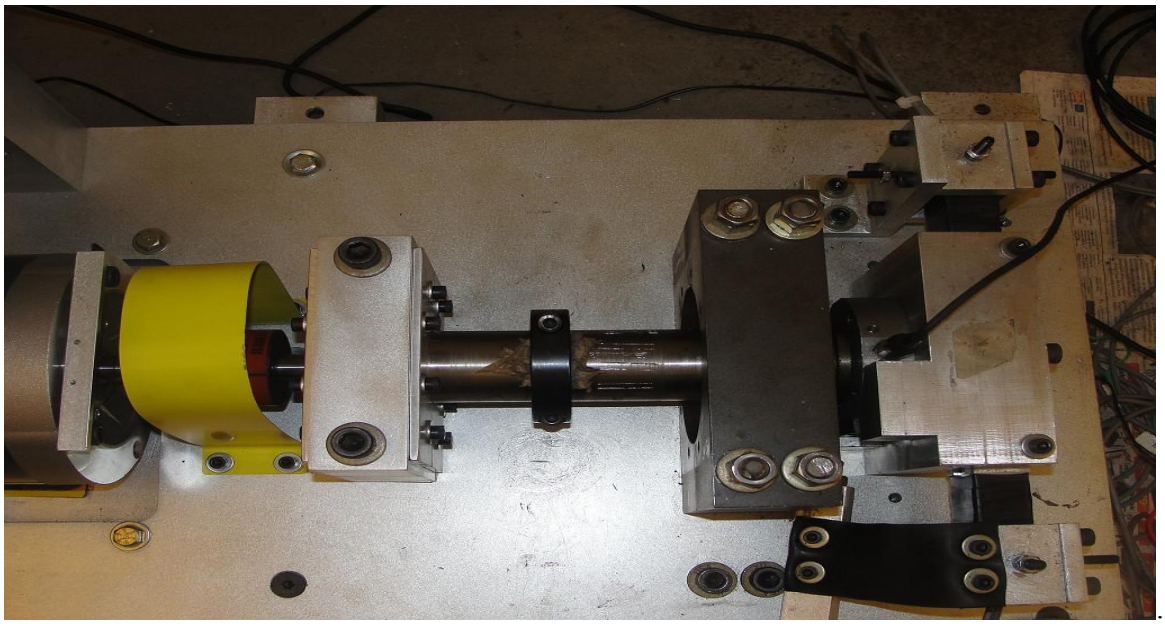

(b)

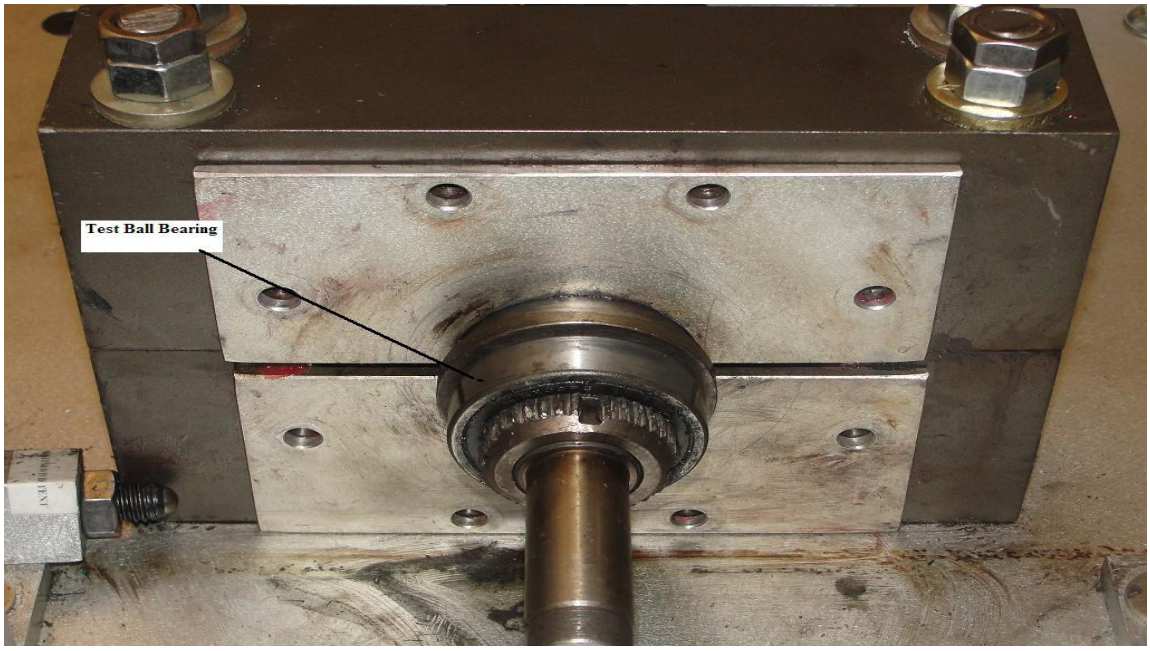

Figure 19 Bearing installation

(a) Related parts. Including shaft, housing and support bearing

(b) The location of test ball bearing

A force column, with a ball end, transfers the load to the housing and creates a force in the radial direction. The direction of the force column is adjusted by pivoting the force alignment adjustment screws. These screws can be adjusted while observing the output of the torque bridge, in Volts. The goal is to minimize the torque bridge output, indicating the force direction is through the shaft center, shown in Figure.20.

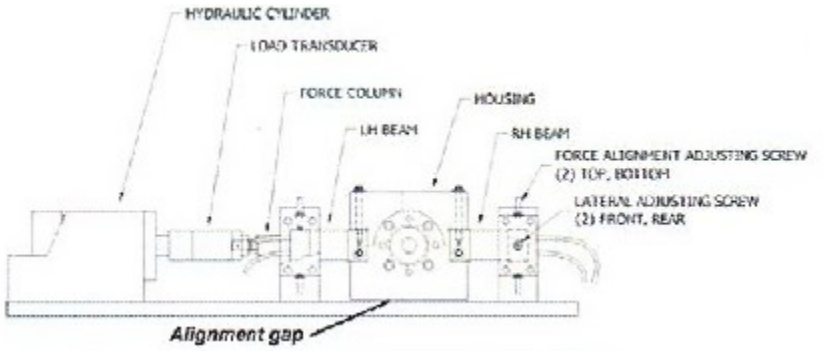

Figure 20 Friction torque system schematic (Spectra Quest, Inc.)

Data acquisition is the process of acquiring signals from test bearings through continuous sampling. In our tests, we collected the vibration signal data using accelerometers. The main purpose of data acquisition of vibration signals is to measure the changes of the object such as test bearing and test environment. The data helps us to detect the spall initiation and monitor the spall propagation process. In case that change occurs, it appears in the form of related vibration motions.

A piezoelectric accelerometer, IMI 608 A11 model sensor, shown in Figure.21, is mounted to the housing which supports the test bearings.

Figure 21　IMI 608 A11 model sensor

A specific equipment, “High speed USB carrier NSI USB-9162”, developed by National Instruments, shown in Figure.22, is used for data collection. The sampling frequency of this unit is 25 KH_z, and thus 25600 data points of vibration amplitude can be collected every second.

Figure 22　High speed USB carrier NSI USB-9162

National Instruments Lab View Signal Express 2009, shown in Figure.23, is used to collect and convert the vibration data. In our test, the vibration data were collected for two seconds every interval. The data processing and data analysis parts are performed using Matlab.

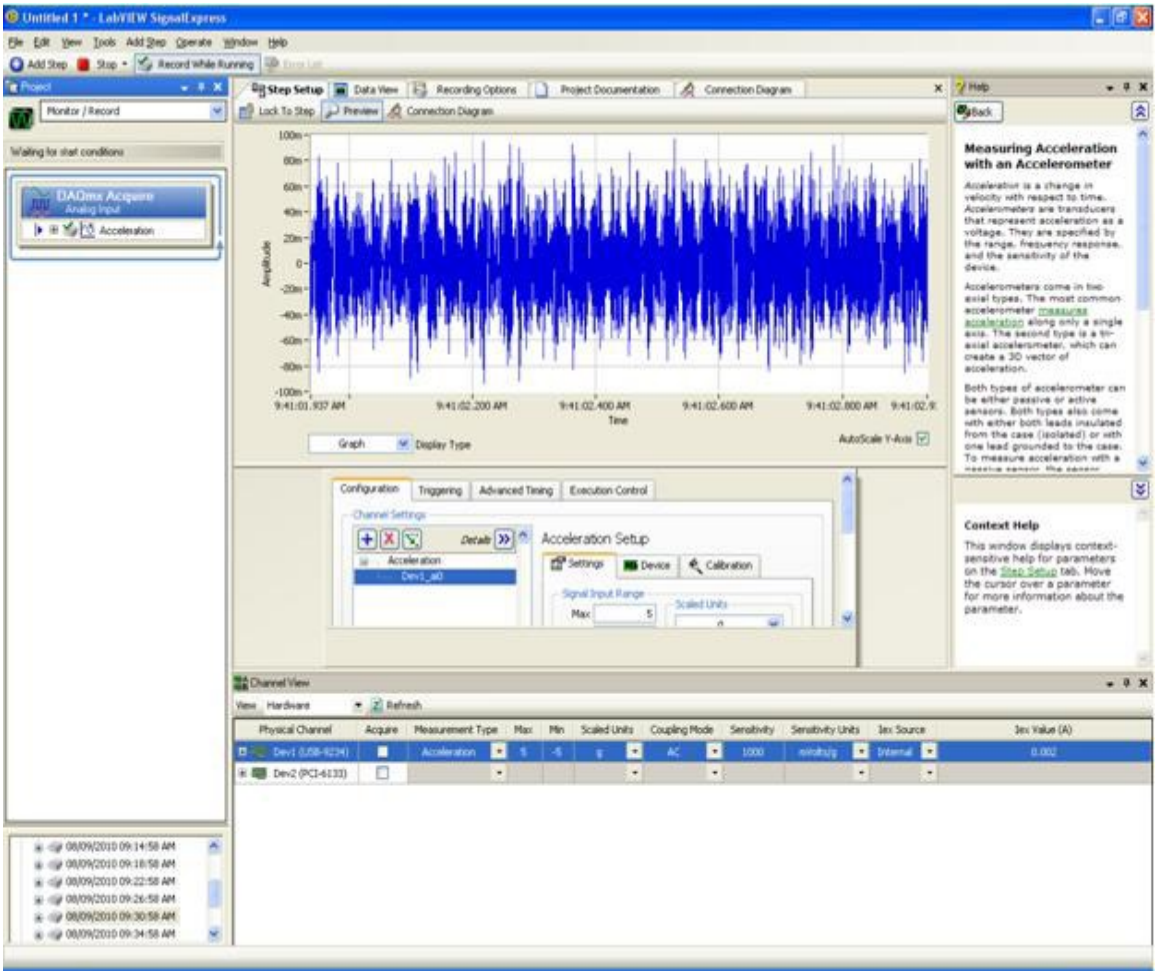

Figure 23 National Instruments Lab View Signal Express 2009

5.3 Experiment Data Analysis

For bearing condition monitoring, effective damage detection algorithm is an important part for data processing and analysis. Therefore, selection of effective plays a vital role for prognostics purposes.

Time domain analysis is used to process the signals. Time domain analysis includes some basic features such as root mean square (RMS), Kurtosis value, Crest factor (CF) value etc.

We used RMS and crest factor value to process our original data. RMS is a common statistical tool which is used to describe the whole process and performance of bearing vibration level. It is the average of the overall vibration level. Therefore, it can detect and record the bearing defect propagation process and be used in different environments, especially in accelerated failure test. The equation of RMS value is.

$$\mathrm{RMS} = \sqrt{\frac{1}{N}\sum_{i=1}^{N} S_i^{\,2}} \tag{5.1}$$

For a whole history data set S, N is the total number of data points and $S_i$is the i_{th} value. However, the limitation of RMS lies in the fact that it is difficult to detect the spall initiation point. RMS is hard to show the change in early stages of bearing degradation. On the other hand, when the defect occurs, higher peak level will increase rapidly because of the short burst of high energy. Meanwhile, the related RMS value doesn't change so quickly.

Peak value of time series data is used to measure the peak amplitude of the signal. In our accelerated life test, peak value shows the slight and sudden changes in vibration amplitudes when spall initiated. The equation of peak value is:

$$\text{Peak Value} = \frac{\max S_i - \min S_i}{2} \tag{5.2}$$

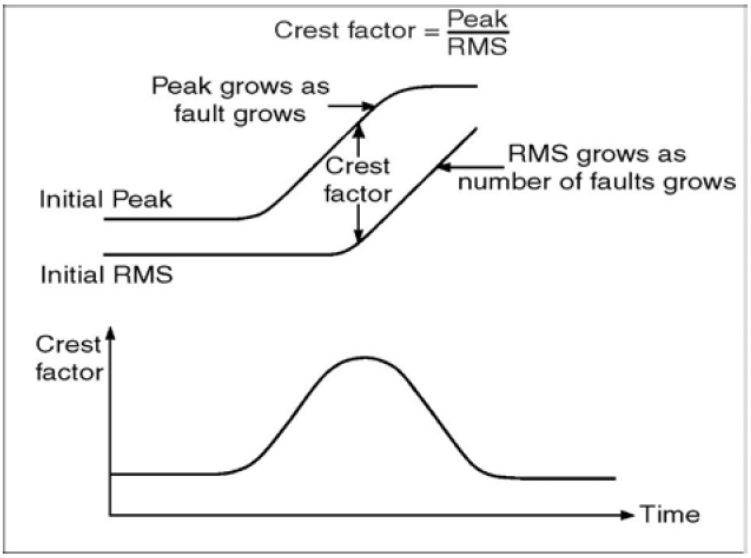

Figure 24 Crest Factor (Bruel&Kjaer Inc)

The crest factor provides us an intuitive result of how much impact exists in the vibration signals. The root cause of the impact is associated with bearing damage. On the other hand, in the early stage, the RMS value only has a slight variation. Thus, as shown in Figure.24, when the damage occurs, the peak value will increase significantly, and the related crest factor will change synchronously. Therefore, as the Peak-to-RMS ratio, the crest factor value is a good indicator when the spall generates. The equation of crest factor is.

$$\text{Crest Factor} = \frac{\text{Peak Value}}{\text{RMS}} \tag{5.3}$$

If we collect the vibration data from undamaged bearings under a normal production environment, the level of crest factor are approximately 3.5. For the vibration data from damaged bearings, the crest factor is more than 6.6. For our experiments, we accelerated this propagation process by high loading and high speed. Therefore, the threshold of de-

fect detection should be different from the normal situation. In order to determine the start point of spall propagation in the experiments, we defined 7.5 as the threshold of spall initiation. This value is obtained by our experiment.

5.4 Experiment 1

The first group of experiments are run-to-failure tests. The conditions of the experiment 1 are shown in Table.10.

Table 10 Test environment and related parameters

Conditions of Experiment	
Load	2500lbf
Temperature	24℃
Rotation Speed	2000RPM
Type of Signal	Vibration
Signal Capture duration	2sec
Data points	51200
Collection Interval	5mins

We monitored the whole propagation process and collected the vibration. The related data such as value of acceleration amplitude, RMS, peak value and crest factor value are shown in the following tables.

As shown in Table.11, a data sample is given.

Table 11 Sample of vibration data

#	1	2	3	4	5	6	…	51200
value	0.0837	0.0691	0.017	0.0352	0.0214	0.0439	…	0.0388

For test #1, the total duration is 9.91 hours. Therefore, there are 119 collection points within the whole process, from the beginning to failure happens. The related values are

shown in Table.12

Table 12 Feature values of test #1

#	1	2	…	64	65	66	……	119
RMS	0.0479	0.0489	…	0.0469	0.0757	0.0478	…	2.3
Peak Value	0.3122	0.2386	…	0.2562	0.5778	0.3252	…	5.1217
CF value	6.5132	4.8751	…	5.4685	7.6347	6.797	…	2.6892

(a)

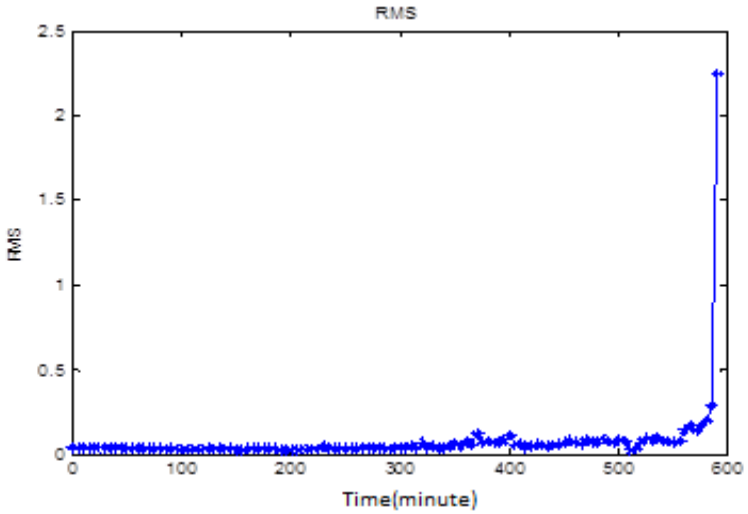

(b)

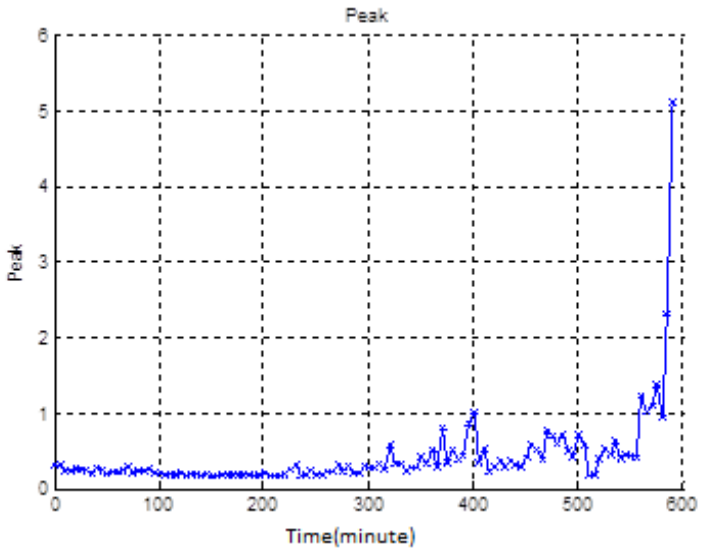

(c)

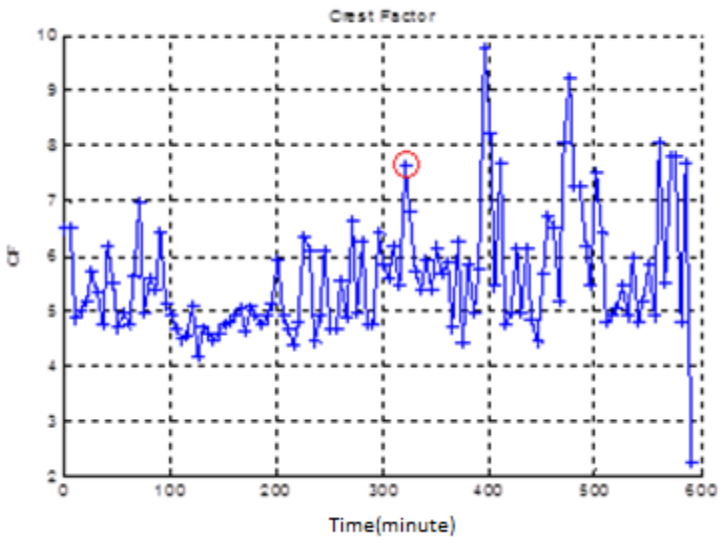

Figure 25 Related features of test #1

(a) RMS value (b) Peak value (c) CF value

As mentioned before, for detection of spall initiation, the threshold value of CF is 7.5.

Based on these CF values shown in Figure 25(c), we can find the spall initiation point #65 (325 minutes). The duration of spall propagation process is 270 minutes.

For Test 2.

Table 13 Feature values of test #2

#	1	2	…	58	59	60	……	177
RMS	0.031	0.0354	…	0.1836	0.175	0.1405	…	0.649
Peak Value	0.1412	0.1697	…	1.6223	1.6259	1.0141	…	3.8657
CF value	4.5521	4.7931	…	8.8392	9.2927	7.2167	…	5.9566

(a)

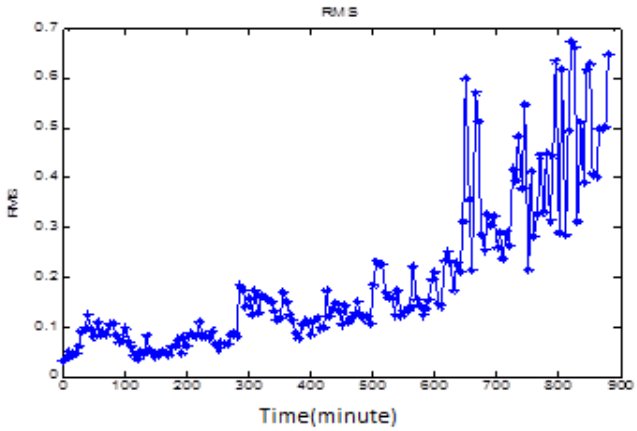

(b)

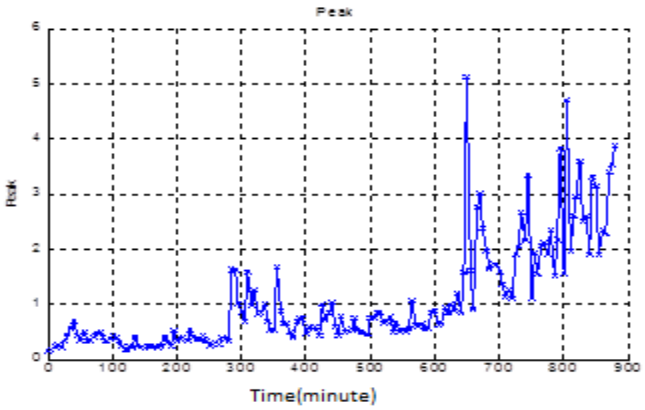

(c)

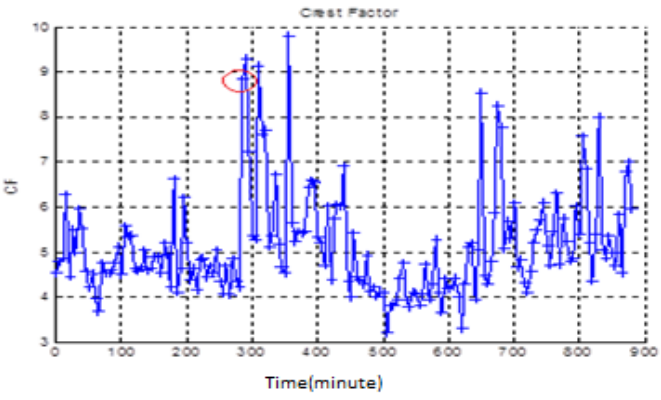

Figure 26 Related features of test #2

(a) RMS value (b) Peak value (c) CF value

Based on CF values, shown in Table.13, we can find the spall initiation point #58 (290 minutes), which is marked in Figure.26(c). The bearing was broken at point #177 (885minutes). For Test 3.

Table 14 Feature values of test #3

#	1	2	…	1182	119	120	……	137
RMS	0.1482	0.1467	…	0.2692	0.3353	0.2736	…	0.6474
Peak Value	0.6959	0.6301	…	0.2562	0.5778	0.3252	…	5.1217
CF value	4.697	4.2967	…	5.2314	7.7967	5.3746	…	7.9118

(a)

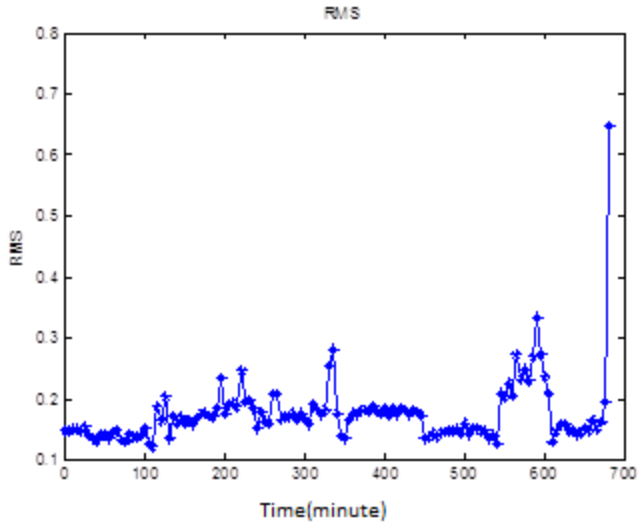

(b)

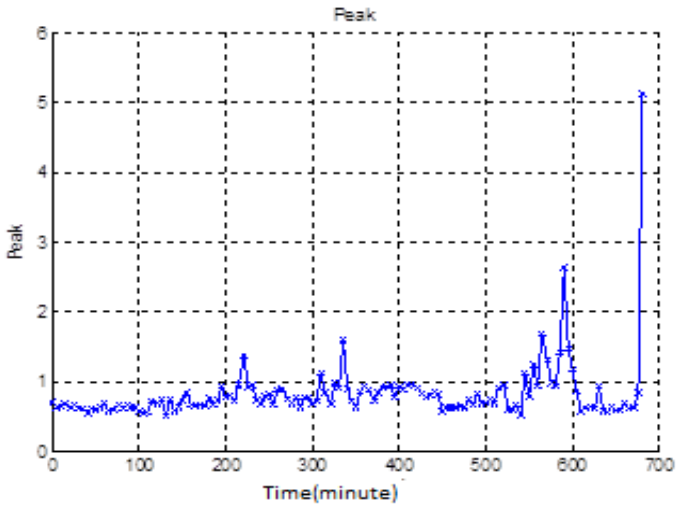

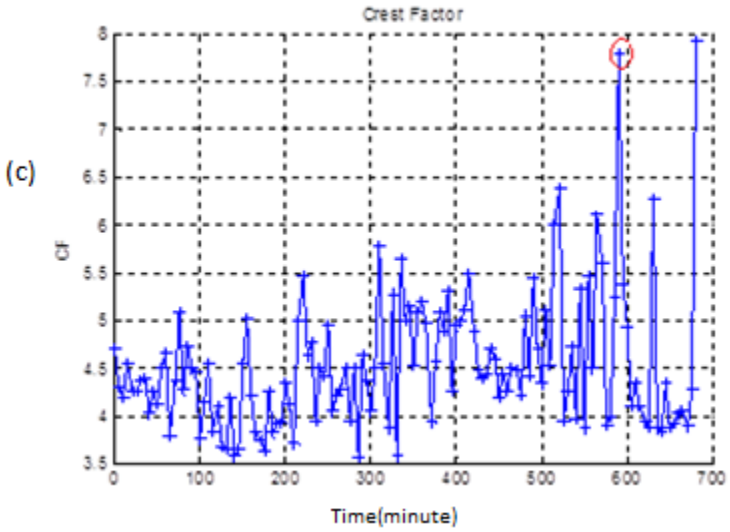

Figure 27 Related features of test #3

(a) RMS value (b) Peak value (c) CF value

Based on CF values, shown in Table.14, we can find the spall initiation point #119 (595 minutes) in Figure.27(c). The bearing was broken at #137 point (685minutes).

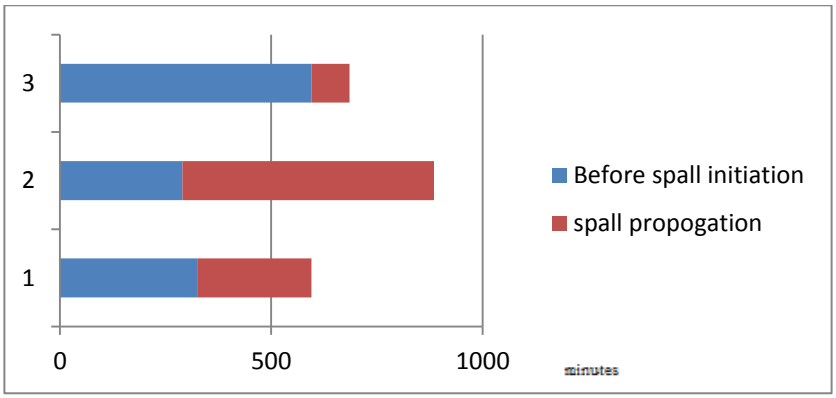

Figure 28 Lifetime of test #1, #2 and #3

Based on the results of these experiments, shown in Figure.28, we can draw a conclusion that different individual bearing may has different propagation processes because of the uncertainties. Therefore, in order to improve the accuracy of the prediction for an individual bearing, we need to consider uncertainties as important factors, and reduce such uncertainties.

5.5 Experiment 2

The main purpose of this experiment is to validate the integrated method discussed before. Firstly, we determine the relationship between signal data and defect value. After data processing, the original vibration data were transformed into RMS data. We assume that there is a linear relationship between these two kinds of data. We can obtain a reasonable value of spall size when we get the related RMS level. Secondly, spall initiation point can be found by monitoring the crest factor value. Then we collected the vibration data and convert it to RMS data during the spall propagation process synchronously. Thirdly, as online condition monitoring data, the related spall sizes are used to adjust model parameter m and narrow down its distribution. Finally, we will test the accuracy of this method by comparing the predictions with values.

Figure 29 showed the whole process. We use related historical data to define the linear parameter of RMS and spall size. The following figures show the change of RMS from spall initiation to the failure. Figure. 30, 31 and 32 show the related RMS of test #1, #2, #3, respectively.

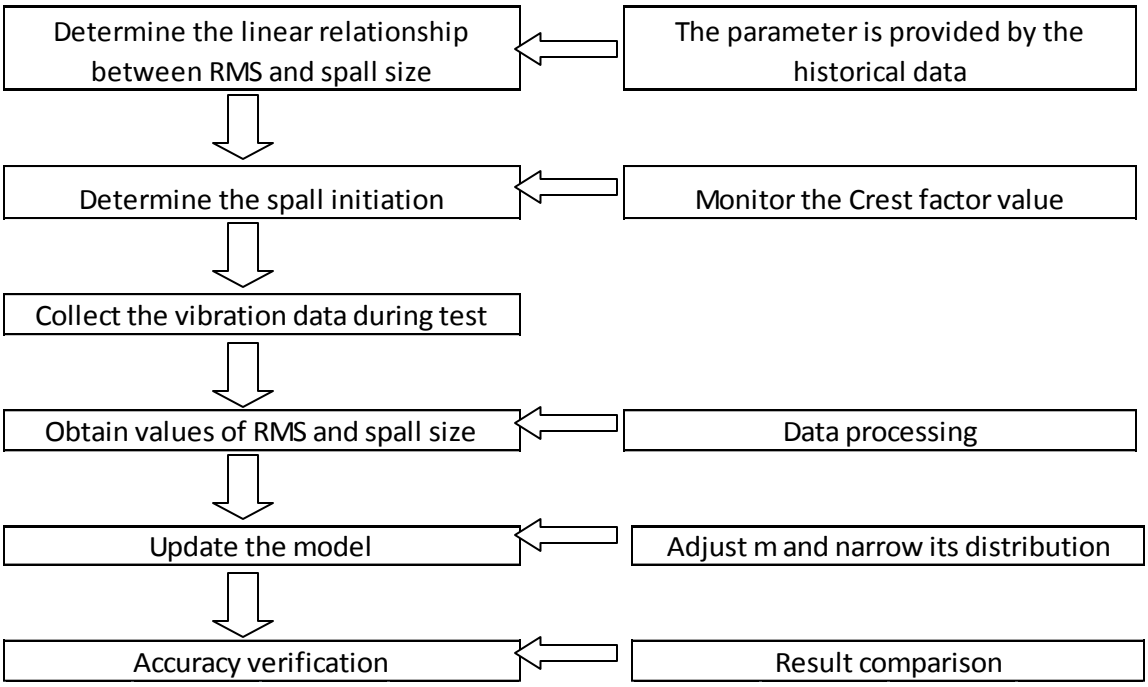

Figure 29 Validation process

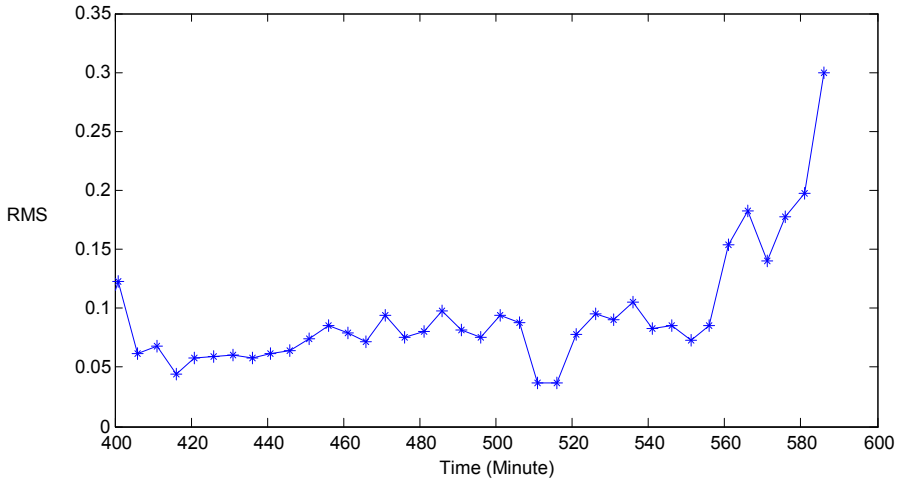

Figure 30 RMS value of test #1

Table 15 Inspection points and related RMS of test #1

Point	81	82	83	84	…	118
RMS	0.08	0.08	0.09	0.12	…	0.3

The spall size at failure point is 15mm² (by measure).

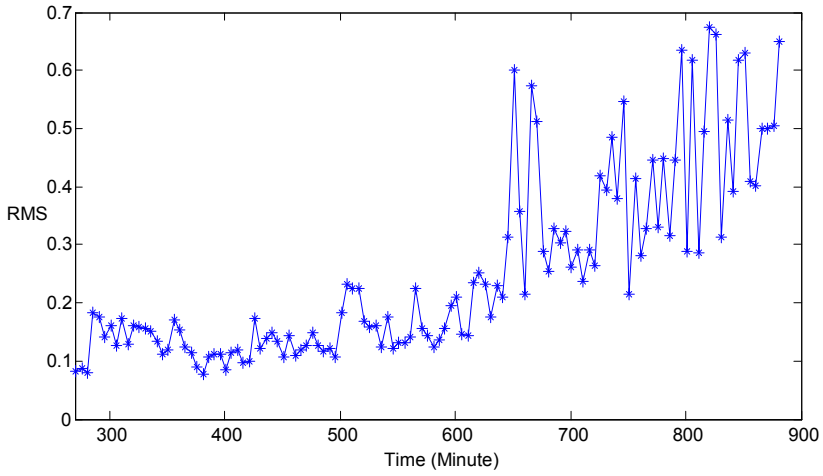

Figure 31 RMS value of test #2

Table 16 Inspection points and related RMS of test #2

Point	53	54	55	56	…	177
RMS	0.07	0.07	0.08	0.08	…	0.65

The spall size at failure point is 30mm².

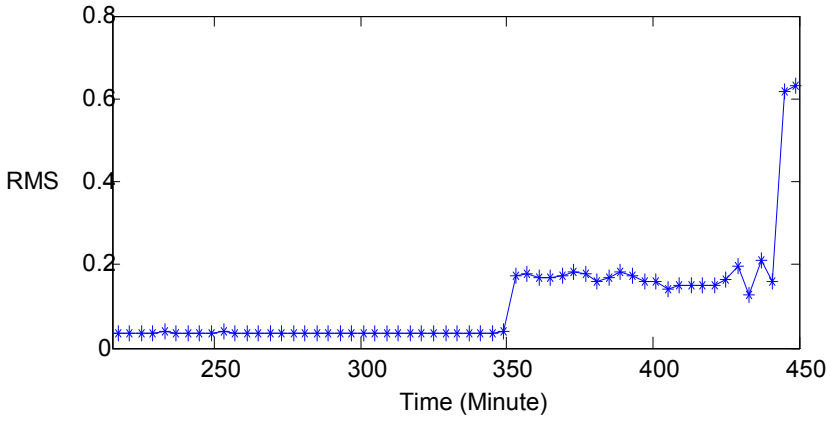

Figure 32 RMS value of test #3

Table 17 Inspection points and related RMS of test #3

Point	53	54	55	56	…	113
RMS	0.05	0.053	0.056	0.071	…	0.631

The spall size at failure point is 28mm², shown in Figure.33. Table.15, 16 and 17 show the RMS levels at different inspection points.

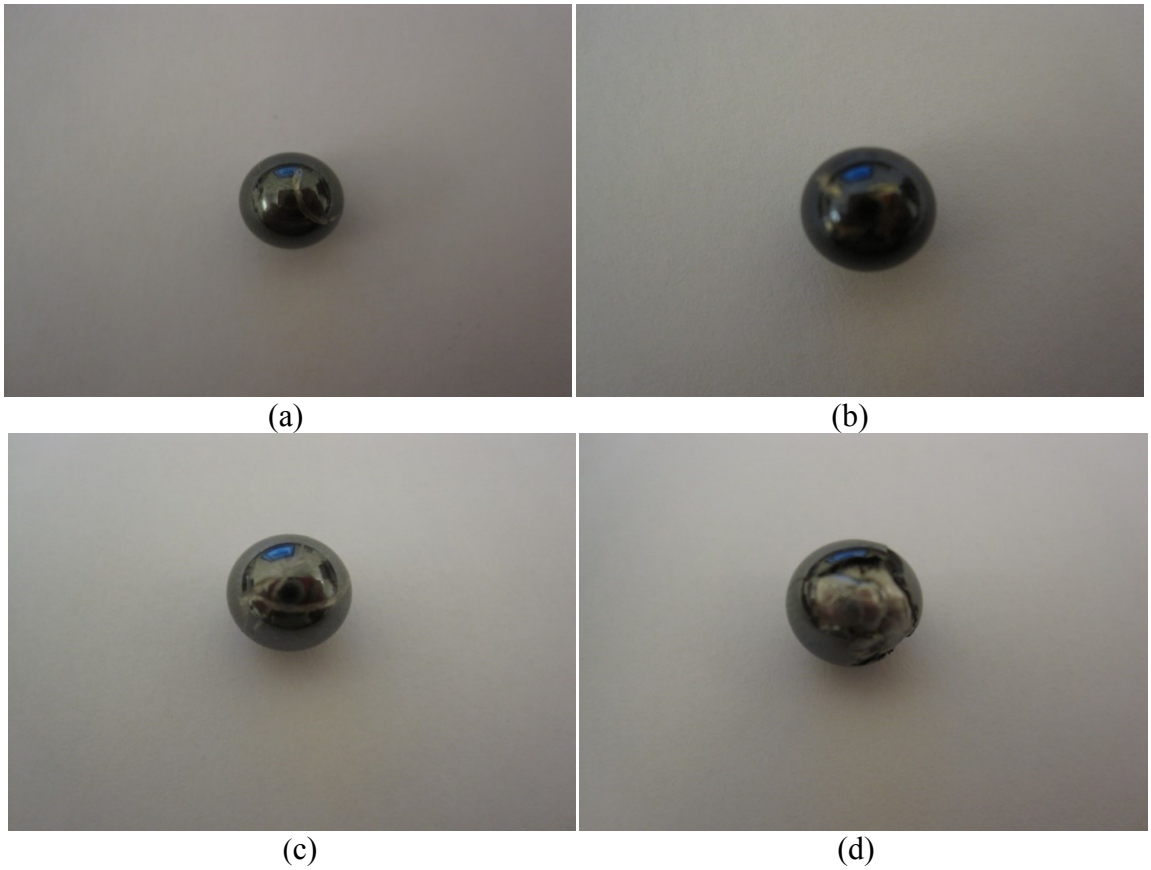

(a) (b) (c) (d)

Figure 33 Spall on the testing balls

(a) (b) (c) (d) spall on different balls

The measured values are shown in the following table, Table.18.

Table 18 Values of RMS and spall size

RMS	0.08	0.07	0.05	0.07	0.05	0.04
Spall size	0.01	0.01	0.01	0.01	0.01	0.01
RMS	0.3	0.65	0.63	0.29	0.64	0.35
Spall size	15	30	28	15	32	16

In order to obtain the linear relationship between these values, we analyzed it by regression model, shown in Figure.34.

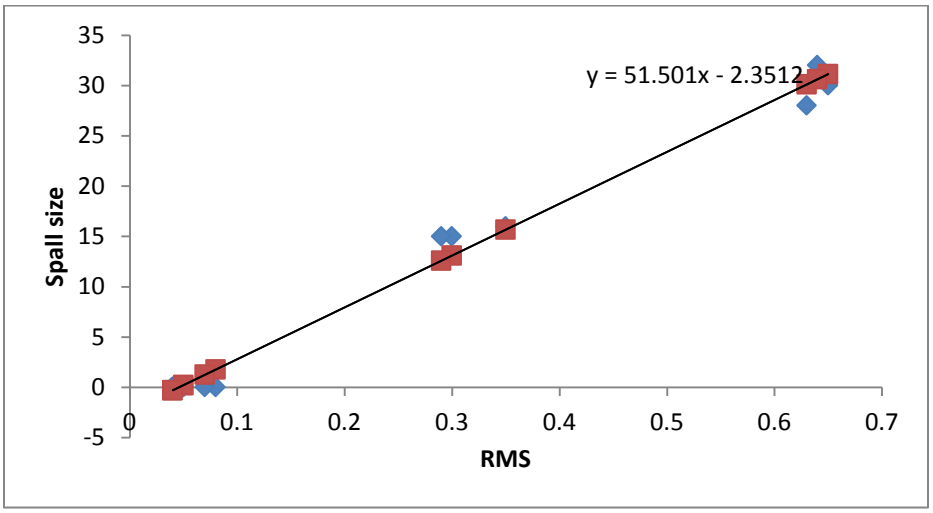

Figure 34 Regression analysis

The linear relationship between spall size and RMS level in our experiment is.

$$Y = 51.501X - 2.3512 \quad (5.4)$$

where Y is spall size, X is RMS level. We used this equation to estimate the spall size in the next step.

5.5.1 Validation test #1

Then we ran new tests at the same condition mentioned above. By monitoring the online crest factor data, we can determine the spall initiation point, #37, shown in Table.19 and Figure.35.

Table 19 CF values until spall initiation

Point	1	2	3	4	…	37
CF	4. 1321	4. 132	3. 9934	4. 4492	…	10. 2642

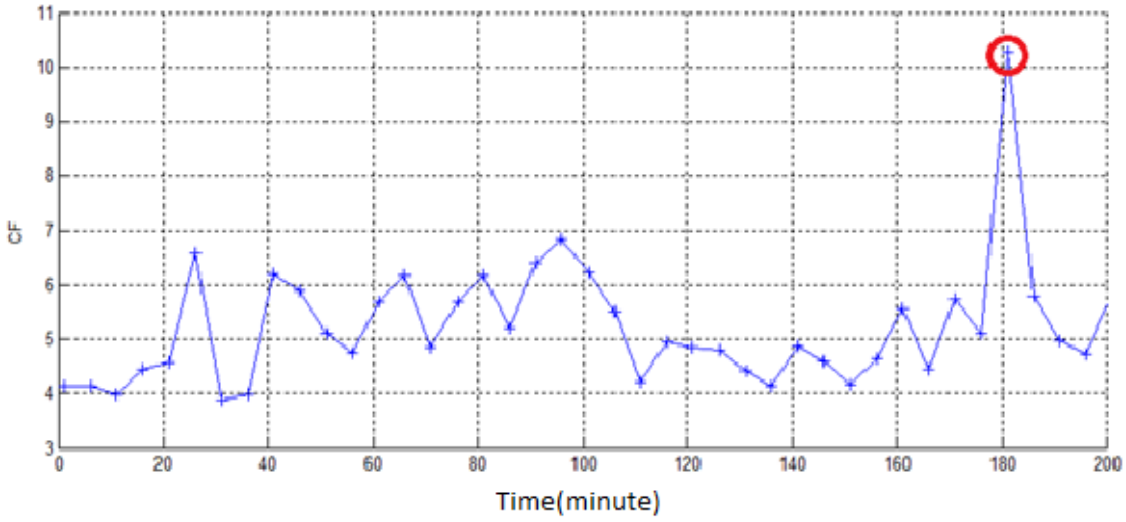

Figure 35 CF values

In spall propagation stage, we collected the vibration signal data every 6e4 cycles, 30 minutes. The RMS and spall size values of these inspection points are shown in Table.20.

Table 20 Related values in the updating process

point	minute	cycle	RMS	spall size
38	0	0.00E+00	0.0363	0.01
44	30	6.00E+04	0.0416	0.01
50	60	1.20E+05	0.042	0.01
56	90	1.80E+05	0.0461	0.0229961
62	120	2.40E+05	0.0508	0.2498108
68	150	3.00E+05	0.0636	0.9051836
74	180	3.60E+05	0.0875	2.1288875
80	210	4.20E+05	0.1273	4.1666873

And then, we updated the mean value of m by Bayes' method. The updating process is shown in Figure.36 and Table.21.

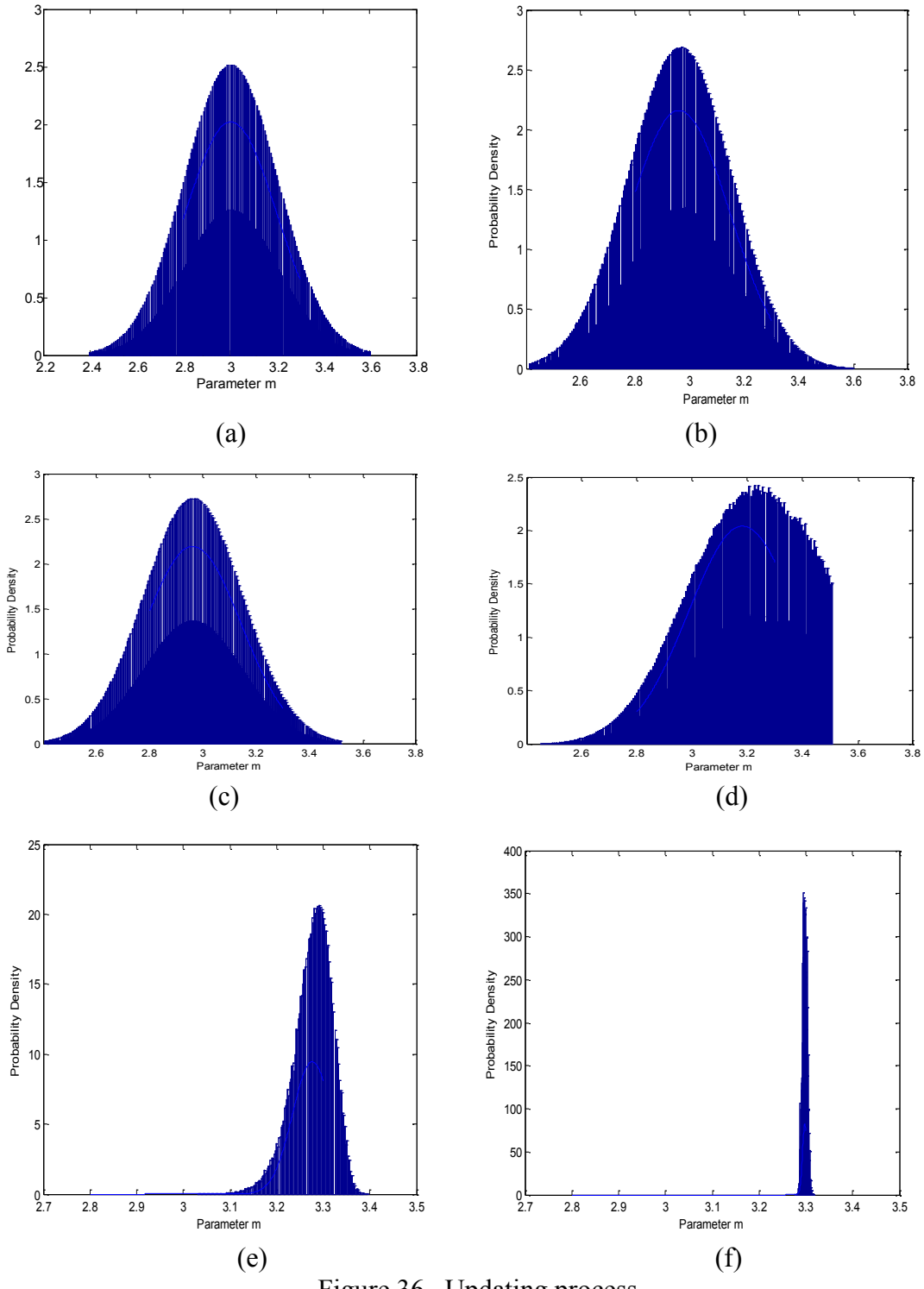

Figure 36 Updating process

(a) 1st update (b) 2nd update (c) 3rd update
(d) 4th update (e) 5th update (f) 6th update

Table 21 Updating date

updating point	loading cycles	spall size	mean of m	std of m
1	6.00E+04	0.01	3	0.2
2	1.20E+05	0.01	3.01	0.197
3	1.80E+05	0.023	2.962	0.185
4	2.40E+05	0.25	2.961	0.182
5	3.00E+05	0.905	3.182	0.095
6	3.60E+05	2.129	3.277	0.042
7	4.20E+05	4.167	3.298	0.005

As a result, the mean value of m was adjusted from 3 to 3.298. And also, from these figures, the distribution of m becomes narrower, and the standard deviation of m is reduced during the updating process. We can use these values and then predict the RUL. The following figure (Figure.37) shows the prediction of RUL.

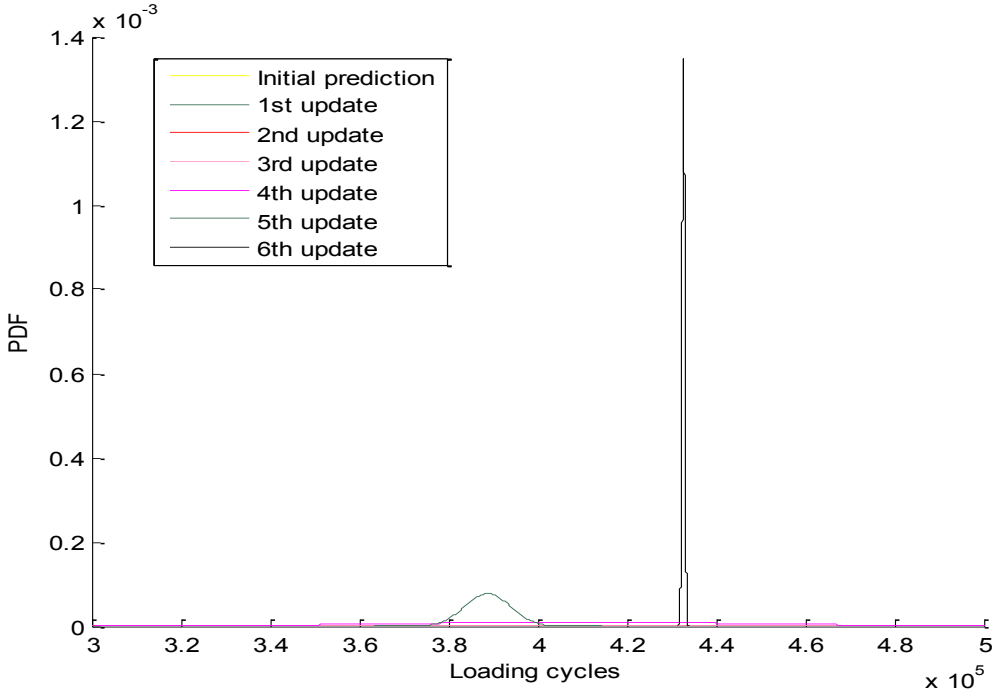

Figure 37 RUL prediction

Table 22 Updated prediction

Point	1	2	3	4	5	6	7
Prediction	1.40E+06	1.50E+06	1.60E+06	1.04E+06	4.28E+05	3.91E+05	4.3E+05

From Table.22, we can see that the final prediction result of RUL is 4.3e5 cycles, equate to 215 minutes. Therefore, the total lifetime of this bearing is 400 minutes.

As discussed before, we can find out failure point by monitoring RMS data. As shown in Figure 38, this test bearing was broken at 415 minutes. The duration of spall propagation process is 230 minutes, from spall initiation to failure. It can be seen that the prediction using our proposed method is very close to the real failure time.

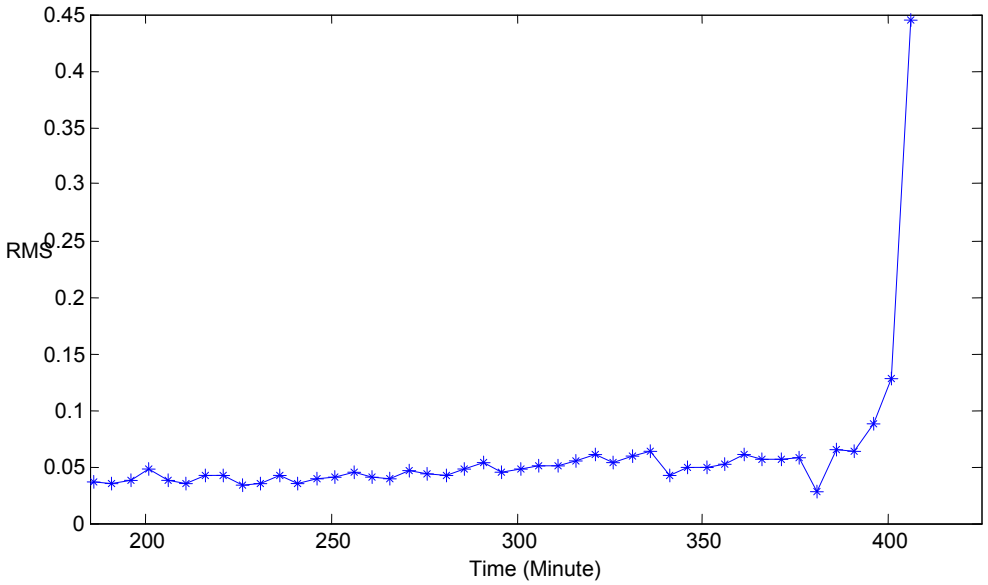

Figure 38 RMS of whole process

5.5.2 Validation test #2

In order to verify the stability and accuracy of this method, more tests are performed. Test

#2 was run under the same condition. This test bearing was broken at 595 minutes. The total time of the whole propagation process was 185 minutes. The result of the prediction is 186 minutes. The results of test #2 are shown in Table.23 and Figure.39.

Table 23 Related values of experiment #2

point	minute	cycle	RMS	spall size
83	0	0.00E+00	0.04446	0.01
89	30	6.00E+04	0.064614	0.944112505
95	60	1.20E+05	0.075077	1.477715235
101	90	1.80E+05	0.087654	2.119161522
107	120	2.40E+05	0.104689	2.987947558
113	150	3.00E+05	0.182683	6.965656073

updating point	mean of m	std of m	Prediction	RUL Time
1	3.264	0.0458	512846.9278	256.4234639
2	3.31	0.0444	470545.5995	235.2727998
3	3.295	0.058	382904.5574	191.4522787
4	3.32	0.036	384709.4808	192.3547404
5	3.35	0.006	371574.1532	185.7870766

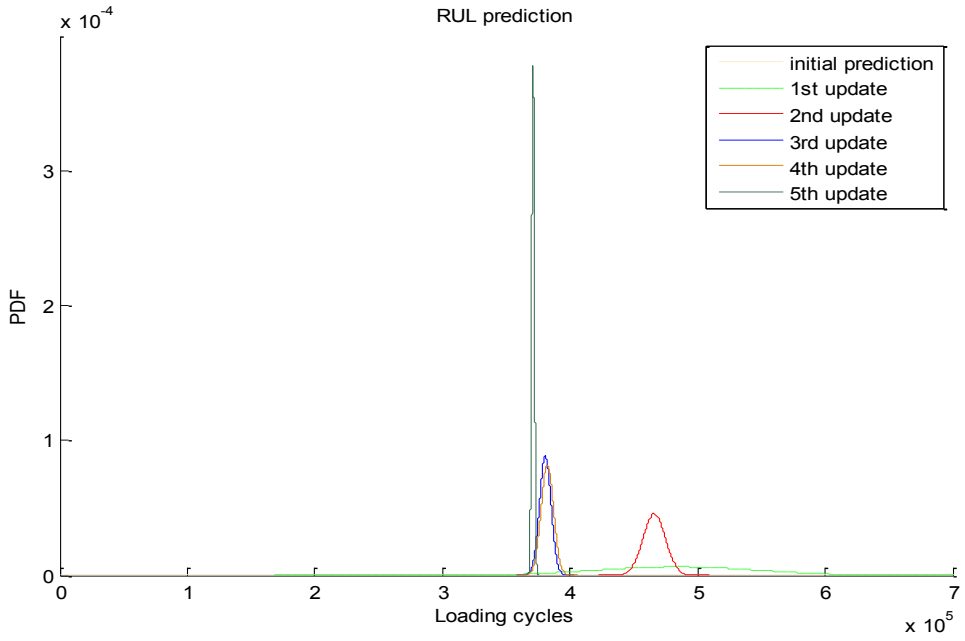

Figure 39 RUL Prediction of experiment #2

In order to compare with traditional model-based methods, we calculate the prediction solely based on the Paris' law model. The results are shown in Table.24.

Table 24 Compare with model-based method

Experiment 1	Prediction	Real RUL	Error rate
Integrated method	215	230	6.50%
Paris' law	175	230	24%
Experiment 2	Prediction	Real RUL	Error rate
Integrated method	186	185	0.50%
Paris' law	175	185	5.40%

Comparing with the normal model-based methods, we find that the integrated method predicts the RUL more accurately. Based on these experiments, we can find that: a) by monitoring CF value, we can determine the spall initial point effectively; b) the experimental results demonstrate that this proposed integrated method can effectively adjust the model parameter based on the on-line data, and lead to more accurate RUL prediction; c) comparing with sole model-based methods, we can obtain more accurate prediction results with this integrated method; d) using this integrated method, an accurate result can be achieved based on limited historical data.

Chapter 6

Conclusions and Future work

6.1 Conclusions

Nowadays, in order to improve the productivity and quality, more and more resources are invested in maintenance. In order to improve the reliability of an engineering system, accurate predictions of the remaining useful lifetime of the equipment and its key parts are required. Bearing plays an important role in the rotating machines. The purpose of using a bearing is to reduce rotational friction and support the load imposed on it in radial and axial directions.

The common types of bearing defects include damage in rolling elements, inner and outer races, etc. In this thesis, we focus on the spall propagation caused by rolling contact fatigue. The existing bearing prognosis methods are either model-based or data driven. In this thesis, we develop an integrated bearing prognostics method, which utilizes both physical models and condition monitoring data. In the physical model part, a Hertz contact model is used to analyze the stress developed from the contact point between two curved surfaces which are pressed together, the ball and the deep groove. Based on Paris' law, a damage propagation model is used to describe the spall propagation process. It is difficult to measure a defect size when the machines are running. Therefore, online data is obtained and processed to transform raw signals into useful information. In this thesis, the uncertainty factors are considered, including material uncertainty, model uncertainty and measurement error. A Bayesian method is used to update the distribution of this uncertainty factor by fusing the condition monitoring data, to achieve refined predictions of

remaining useful life.

Finally, two sets of data are used to verify and validate the proposed integrated bearing prognostics method. The first set of data includes a group of simulated bearing degradation histories. The second set of data were collected from lab experiments conducted using the Bearing Prognostics Simulator. These examples demonstrated the effectiveness of the proposed method.

The key contribution of this thesis is the development of an integrated bearing prognostics method, where the uncertain model parameters are updated using the collected condition monitoring data, while the existing bearing prognostics methods are either model-based or data driven. Both the development of the method and the experimental validation are significant contributions to the field of bearing prognostics.

6.2 Future work

In order to improve the performance of this integrated bearing prognostics method, several further studies can be conducted as follows:

- In this thesis, we mainly use CF value to detect the spall initiation time. This method can only be used in a relative ideal environment, such as laboratory environment. Thus, the function of this detection method is limited in a real production environment. It is necessary to develop a more accurate and comprehensive method for detection of bearing fault initiation time
- In this thesis, we have not investigated the fault type of the bearings via signals.

We can further develop methods for detection of bearing fault types.

- In this thesis, we obtain the actual spall size by relating it to vibration RMS values, and consider the related measurement uncertainty. In future work, more experimental data such as spall size values at different time should be obtained in a more accurate way. Some more precise methods such as X-ray or heat-imaging may be used to collect these data.
- In order to expand the use of this integrated prognostics method, we will investigate this approach under varying load and speed.

References

[1] Dyer. D., & Stewart, R. M, Detection of Rolling Element Bearing Damage by Statistical Analysis. *ASME J. Mech. Des, Vol.* 100, 229–235, 1978

[2] Price, E.D, A. W. Lees, & Friswell, M. I, Application of High Frequency Monitoring for classification of Rolling Element Bearing Failures. *Key Engineering Materials Vols*. 204-205, 173-182, 2001

[3] Khemili, I., & M. Chouchane, Detection of Rolling Element Bearing Defects by Adaptive Filtering. *European Journal of Mechanics A/Solids, Vol*. 24, 293-303.2005

[4] Chaudhary. A. & Tandon.N, A Theoretical Model to Predict Vibration Response of Rolling Bearings to Distributed Defects under Radial Load. *Journal of Vibration and Acoustics, Transactions, ASME, Vol*.120, 214-220, 1997

[5] Lewis Rosado, Nelson H. Forster, Kevin L. Thompson & Jason W. Cooke, Rolling Contact Fatigue Life and Spall Propagation of AISI M50, M50NiL, and AISI 52100, Part I: Experimental Results, Tribology Transactions, 53:1, 29-41,2009

[6] Nagaraj K. Arakere, Nathan Branch, George Levesque, Vaughn Svendsen & Nelson H. Forster, Rolling Contact Fatigue Life and Spall Propagation of AISI M50, M50NiL, and AISI 52100, Part II: Stress Modeling, Tribology Transactions, 53:1, 42-51,2009

[7] Nelson H. Forster, Lewis Rosado, William P. Ogden & Hitesh K, Trivedi, Rolling Contact Fatigue Life and Spall Propagation Characteristics of AISI M50, M50 NiL, and AISI 52100, Part III: Metallurgical Examination, Tribology Transactions, 53:1, 52-59,2009

[8] Y. Li, S. Billington, C. Zhang, T. Kurfess, S. Danyluk, S. Liang, Adaptive prognostics for rolling element bearing condition, Mechanical Systems and Signal Processing 13 103–113, 1999

[9] Y. Li, T.R. Kurfess, S.Y. Liang, Stochastic prognostics for rolling element bearings, Mechanical Systems and Signal Processing 14 747–762, 2000

[10] G.J. Kacprzynski, A. Sarlashkar, M.J. Roemer, A. Hess, B. Hardman, Predicting remaining life by fusing the physics of failure modeling with diagnostics, JOM Journal of the Minerals, Metals and Materials Society 56 29–35, 2004

[11] C.J. Li, H. Lee, Gear fatigue crack prognosis using embedded model, gear dynamic model and fracture mechanics, Mechanical Systems and Signal Processing 19 836–846, 2005

[12] R. Orsagh, M. Roemer, J. Sheldon, A comprehensive prognostics approach for predicting gas turbine engine bearing life, Proceedings of the 10th National Turbine Engine High Cycle Fatigue Conference, New Orleans, LO, 2004.

[13] J. Qiu, B.B. Set, S.Y. Liang, C. Zhang, Damage mechanics approach for bearing lifetime prognostics, Mechanical Systems and Signal Processing 16 817–829, 2002

[14] C.H. Oppenheimer, K.A. Loparo, Physically based diagnosis and prognosis of cracked rotor shafts, Proceedings of SPIE Component and Systems Diagnostics, Prognostics, and Health Management II, Bellingham, pp. 122–132, 2002

[15] Tian, Z. An Artificial Neural Network Method for Remaining useful Life Prediction of Equipment Subject to Condition Monitoring. *Journal of Intelligent Manufacturing,*, pp:1-6. 2009

[16] P. Wang, G. Vachtsevanos, Fault prognostics using dynamic wavelet neural networks, Artificial Intelligence for Engineering Design, Analysis and Manufacturing 15 349–365. 2001

[17] W.Q.Wang, M.F. Golnaraghi, F. Ismail, Prognosis of machine health condition using neuro-fuzzy systems, Mechanical Systems and Signal Processing 18 813–831,2004

[18] Tian. Z, Lorna, W, & Nima, S, A Neural network Approach for Remaining useful Life Prediction utilizing both Failure and Suspension Histories. *Mechanical Systems and Signal Processing, Vol*.24, 1542-1555 ,2010

[19] N. Gebraeel, M. Lawley, R. Liu, V. Parmeshwaran, Residual life predictions from vibration-based degradation signals: a neural network approach, IEEE Transactions on Industrial Electronics 51 694–700, 2004

[20] E. Jantunen, Prognosis of rolling bearing failure based on regression analysis and fuzzy logic, Proceedings of the VETOMAC-3 and ACSIM-2004, New Delhi, India, pp. 836–846, 2004

[21] S. Zhang, L. Ma, Y. Sun, J. Mathew, Asset health reliability estimation based on condition data, Proceedings of the 2nd WCEAM and the 4th ICCM, Harrogate, UK, pp. 2195–2204,2007

[22] X. Zhang, R. Xu, C. Kwan, S. Y. Liang, Q. Xie, L. Haynes, An integrated approach to bearing fault diagnostics and prognostics, Proceedings of American Control Conference, Portland, OR, USA, pp. 2750–2755, 2005

[23] K.B. Goode, J. Moore, B.J. Roylance, Plant machinery working life prediction method utilizing reliability and condition-monitoring data, Proceedings of Institution of Mechanical Engineers 214 109–122, 2000

[24] Jardine, A., Lin, D., & Banjevic, D. A Review on Machinery Diagnostics and Prognostics Implementing Condition-Based Maintenance. *Mechanical System and Signal Processing, Vol.20, 1483-1510, 2006*

[25] A.K.S. Jardine, Maintenance, replacement and reliability, Wiley, New York, 1973.

[26] A.K.S. Jardine, P.M. Anderson, D.S. Mann, Application of the Weibull proportional hazards model to aircraft and marine engine failure data, Quality and Reliability Engineering International 3 77–82. 1987

[27] A.K.S. Jardine, P. Ralston, N. Reid, J. Stafford, Proportional hazards analysis of diesel engine failure data, Quality and Reliability Engineering International 5 207–216, 1989

[28] Y. Sun, L. Ma, J. Mathew, W. Wang, S. Zhang, Mechanical systems hazard estimation using condition monitoring, Mechanical Systems and Signal Processing 20 1189–1201, 2006

[29] W. Wang, A model to predict the residual life of rolling element bearings given monitored condition information to date, IMA Journal of Management Mathematics 13 3–16, 2002

[30] W.Wang,W. Zhang, A model to predict the residual life of aircraft engines based upon oil analysis data, Naval Research Logistics 52 276–284, 2005

[31] Satish, B., & Sarma, N.D.R, A Fuzzy BP Approach for Diagnosis and Prognosis of Bearing Faults in Induction Motors*, IEEE Power Engineering Society General Meeting, vol.* 3, 2291–2294, 2005

[32] Wu, S. J., Gebraeel, N., Lawley, M. A., & Yih, Y, A Neural Network Integrated Decision Support System for Condition-Based Optimal Predictive Maintenance Policy. *IEEE Transactions on Systems Man and Cybernetics, Vol*. 37, 226–236, 2007

[33] Tian, Z. An Artificial Neural Network Method for Remaining useful Life Prediction of Equipment Subject to Condition Monitoring. *Journal of Intelligent Manufacturing,*, pp:1-6, 2009

[34] Tedric A. Harris, Michael N. Kotzalas, Rolling Bearing Analysis, Fifth Edition, 2006

[35] Yu, and Harris, "A New Stress-Based Fatigue Life Model for Ball Bearings", Tribology Transactions, Vol. 44, pp. 11-18, 2001

[36] Michael J Gregory J and Rolf F, Advanced Vibration Analysis to Support Prognosis of Rotating Machinery Components, 2008

[37] Sean Marble and Brogan P, Predicting the Remaining Life of Propulsion System bearing, IEEE Aerospace Conference. 2006.

[38] Li, Y., Billington, S., Zhang, C., Kurfess, T., Danyluk, S., and Liang, S., Dynamic Prognostic Prediction of Defect Propagation on Rolling Element Bearings, Tribol. Trans., 42, No. 2, pp. 385–392. 1999

[39] Lundberg, G and Palmgren, A, Dynamic Capacity of Rolling Bearings. Acta Polytech, Mech Engr, Ser, 1 pp 1-50 1947

[40] Vingsbo, O., and Qsterlund,R, Phase Changes in Fatigues Ball Bearings. Metallurgical Transactions A 11A,pp 701-707, 1980

[41] Kptzalas M and Harris, T.A, Fatigue Failure Progression in Ball Bearings. Trans. ASME,123,pp 238-242, 2001

[42] Jones, A.B. The Life of High-Speed Ball Bearings. *ASME Trans.*, **74**, pp 695-703, 1952

[43] Ioannides, E. and Harris, T.A, A New Fatigue Life Model for Rolling Bearings. *J. Trib*., 107, pp 367-378. 1985

[44] M.Kuna, M. Springmann, K madler, P Hubner,G Pusch, Fracture mechanics based design of a railway wheel made of austempered ductile iron. Engineering Fracture Mechanics 72 pp. 241-253 2005

[45] Xu, G. and Sadeghi, F. Spall Initiation and Propagation Due to Debris Denting. *Wear*, 201, pp 106-116, 1996

[46] Shao,Y., & Nezu, K. Prognosis of Remaining Bearing Life using Neural Networks. *Proc Instn Mechanical Engineers, Vol.* 214, 217-230,2000

[47] Utah University. Precision Machine Design. Retrieved from http://www.mech.utah.edu/~me7960/lectures/Topic7-ContactStressesAndDeformations.pdf

[48] SKF Canada limited. Retrieved from http://www.skf.com/ca/en/products/bearings-units-housings/ball-bearings/deep-groove-ball-bearings/index.html

[49] Bruel&Kjaer, Inc. Detecting Faulty Rolling Element Bearings. Retrieved from http://www.bkvibro.com/fileadmin/mediapool/Internet/PDF-Files/Publications/Application_Notes/detecting_faulty_rolling_element_bearings.pdf

[50] Spectra Quest Inc. Retrieve from http://spectraquest.com